# QUARKONIUM AND QUARK LOOPS*

By N. A. Törnqvist

Department of High Energy Physics, University of Helsinki, Siltavuorenpenger 20 C, SF-00170 Helsinki 17, Finland

*(Received October 29, 1984)*

We review some recent work on quarkonium and discuss in particular how naive models can be improved to include nonperturbative quark loops phenomenologically using the unitarized quark model. We argue that such nonperturbative loops which are required by unitarity and finite widths play an important rôle in shifting hadron masses by up to 100's of MeV, generating considerable resonance mixings and higher Fock space (multi--quark) components in hadron wave functions. Many effects currently often ascribed to gluon exchange alone can also be described by quark loops. Allowing for a smaller $\alpha_s$ in bound states nonperturbative quark loops could e.g., resolve the puzzle of absence of the $\vec{L} \cdot \vec{S}$ term in baryon spectroscopy. Even for the heavy upsilon states the mass shifts are as large as up to 80 MeV — and in particular the 5S mass, being above the $B\bar{B}$ threshold provides a sensitive test to these ideas.

PACS numbers: 11.15.–q, 11.15.Ha, 12.35.Eq

CONTENTS



---

* Presented at the XXIV Cracow School of Theoretical Physics, Zakopane, June 6–19, 1984.

## *1. Introduction*

"The difficulty of physics is to see its simplicity"

The quark model of hadronic particles is only twenty years old [1–3]. During these years high energy physicists have gathered a strong collective conviction that the hadrons are built from quarks bound together by gluonic forces. Thus although the quarks in the very beginning were met with skepticism, and although they never have been seen as free particles, they are by now very well established.

In the meantime our understanding of strong interactions has undergone something of a revolution. In the sixties and early seventies no respectable author would have claimed that we have a good theory of strong interactions, in spite of the many successful models, mechanisms and phenomenological analyses of data that were then introduced. Today almost the opposite is true; many authors believe that the fundamental dynamical theory is that of quarks interacting through coloured gluons as prescribed by QCD, in spite of the fact that very few and only qualitative "QCD inspired" tests can be made. Because of the complexity of the theory and in particular because of the problem of confinement, which generally is put in by hand, a true QCD solution for evaluating the mass spectrum of hadrons is not feasible at present. Therefore present attempts to understand e.g. hadron masses really rely on guesses or heuristic arguments of what the authors believe to be the dominant effects.

Thus most present theoretical hadron spectroscopy is based upon QCD inspired generalizations of the effects well known from the hydrogen atom; only the parameters and the form of the potential is different. For heavy quarks at least this seems to be a good first approximation to the actual situation. But, with a few exceptions, current models neglect the unitarity effects, which must be present in any theory, and which already in the early days of the quark model were believed to be crucial [4–6].

Through unitarity one introduces loop diagrams to be added to the hadron mass matrix. In terms of QCD this means quark loops. These can be divided into two classes: (*i*) perturbative quark loops which, when neglecting quark masses, can be summed and

absorbed into a running coupling constant and (*ii*) non-perturbative quark loops which depend on details of threshold positions, hadronic wave functions etc. The latter effect gives rise to $s$-channel cuts in the mass matrix, with the associated finite widths of resonances corresponding to second sheet poles. These cuts are nearby singularities, which through the associated dispersive (real) parts contribute to hadronic mass shifts of physical hadron masses. Such mass shifts must thus be present in any theory, including the true QCD solutions.

To include these mass shifts in an actual calculation is a complicated and laborious matter indeed, which necessarily involves some phenomenology related to hadronic form factors or wave functions. Therefore they are often neglected hoping that they are not very large.

The following simple and almost model independent argument shows, however, that they should be large: typical (OZI allowed) hadronic width is $\gtrsim 100$ MeV for a resonance lying $\gtrsim 100$ MeV above the first threshold (e.g. $\Delta \to N\pi$). I.e. the variation in the imaginary part of the mass matrix ($M$) with energy ($\sqrt{s}$) is about 0.5 above threshold:

$$\frac{d}{d\sqrt{s}}(-\operatorname{Im} M(s)) \approx \frac{\frac{1}{2}\Gamma}{m_r-(m_1+m_2)} \approx 0.5. \tag{1.1}$$

Below threshold, on the other hand, Im $M$ vanishes. Disregarding "pathological models" (which might be invoked for an individual resonance, but hardly simultaneously for a whole SU6 multiplet or for a group of radially excited states like the upsilons) the real part should near threshold, because of analyticity, on the average have a similar variation with energy:

$$\left|\frac{d}{d\sqrt{s}}(\operatorname{Re} M(s))\right| \approx 0.5. \tag{1.2}$$

This implies a large dependence of the mass shift $\Delta M$ on resonance position. E.g. a state near threshold can be shifted by $\approx 50$ MeV more than a similar state $\approx 100$ MeV below the threshold. Since we must add the contributions from many different thresholds the total relative mass shift can be larger than this. Thus one is led to hadronic mass shifts of the same order of magnitude as the typical SU6 breaking in the hadron mass spectra. Clearly they cannot be neglected; they could even be the dominant effect.

A few words of caution should be mentioned: For a single isolated resonance a mass shift can always be absorbed by renormalization into the bare parameters of the theory, in particular into the definition of the "bare mass". Then of course the mass shift loses its meaning; or alternatively models can be built where a mass shift is small or vanishes. On the other hand in the explicit models we discuss below the overall shift ($\Delta M$) will generally be quite large (up to 1 GeV! for light hadrons and even $\sim 70$ MeV for upsilons) and will depend on details of the model (in particular the hadron size giving the effective cutoff). The over all mass shift is however not very interesting since it can always be absorbed into renormalized quark masses. Therefore the effect on mass splittings ($K^*-K$, $\Delta-N$, $\Upsilon(NS)$

$-\Upsilon((N-1)S)$ etc.), which effectively depend on the derivative $\frac{d}{d\sqrt{s}}(\Delta M)$ is much more interesting and much less sensitive to such details.

In the following we shall first shortly review in Section 2 the experimental situation and comment on current models, which generally are not unitary. In Section 3 we discuss some simple analytic properties of perturbative fermion loops in QED and QCD and in Section 4 we discuss the $^3P_0$ model for hadron decays. Sections 5–6 are the central sections of this paper. In Section 5 we discuss how to unitarize the quark model, i.e. how to include phenomenologically the quark loops. In Section 6 we compare with experimental data. Some of these results have also been published previously, for light quarkonium see Refs [7–12], heavy quarkonium [13–15] and baryons [16–18]. Finally in Section 7 we make some concluding remarks.

## 2. *Comments on the experimental situation, naive potential models, "soft" and "quenched" QCD*

### 2.1. The experimental quarkonium mass spectra

Let us first review shortly the present experimental situation and some conventional models where unitarity effects are neglected. The well known 1S and 1P wave light and $c\bar{c}$ quarkonium states are shown in Fig. 1. The naivest model of simply adding constituent quark masses ($m_u \approx m_d \approx 380$ MeV, $m_s - m_u \approx 125$ MeV and $m_c - m_u \approx 1100$ MeV) is very crude and works only for the vector mesons (and reasonably well for the tensor

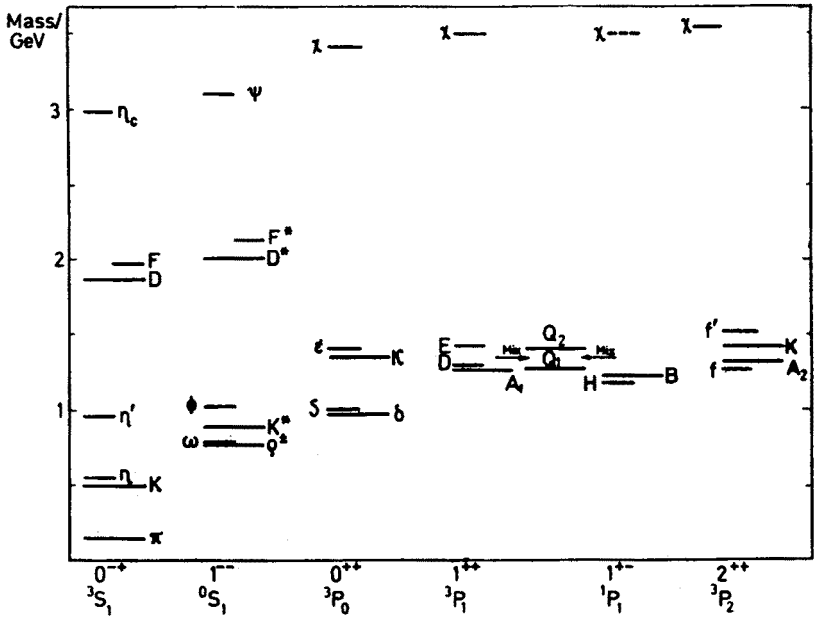


Fig. 1. The experimentally known 1S and 1P light and charm quarkonium states. Missing from complete multiplets are the $s\bar{s}$ $1^{+-}$ state (H′) and the charmed, ($c\bar{u}$, $c\bar{d}$ and $c\bar{s}$) P wave states as well as the $c\bar{c}$ $1^{+-}$ state

mesons if $m_u$, $m_d$ are increased). However, such a quark counting model is still useful as a simple reference model since it is convenient to discuss the actual deviation from such a simple model. We note in particular: (*i*) the $I = 0$, $I = 1$ degeneracy is broken and that sometimes the isosinglet is heavier ($0^{-+}$, $1^{--}$, $1^{++}$) and sometimes the reverse is true ($2^{++}$, $1^{+-}$), without any obvious systematic reason, (*ii*) the lighter the meson the larger are the deviations from the naive quark counting model; in particular the effective strange–nonstrange quark mass splitting and the deviation from ideal mixing increases with decreasing meson mass, (*iii*) the axial strange mesons $Q_1$, $Q_2$ are, due to SU3 breaking, nearly $45^0$ mixtures of the naive states, (*iv*) the light scalar mesons behave anomalously; the $s\bar{s}$ state (S(975)) is much too light, the $s\bar{u}$ state ($\kappa(1350)$) is much too heavy and the $\varepsilon$ is a broad structure with large mass while the $\delta$ is much narrower than SU3 would predict.

In heavy quarkonium the flavour multiplet structure is less interesting, but instead we have many radial excitations. For the upsilons we have three $1^{--}$ states below the $B\bar{B}$ threshold and three above. This is of particular interest to our model since the $B\bar{B}$ etc. threshold effects can be studied in detail.

For a detailed recent review on experimental meson spectroscopy see Ref. [19].

## 2.2. "Soft QCD"

Before we embark on the discussion of quark loops and unitarity effects, let us shortly review current models which neglect these effects. The most detailed such model is perhaps the "soft QCD" (cf. Ref. [20]) which is essentially a generalization of the highly successful model for the hydrogen atom to quarkonium. For some recent reviews see Refs [21–22].

In the soft QCD framework one solves a (single channel) Schrödinger equation

$$H\psi = (H_0 + V)\psi = E\psi, \tag{2.1}$$

where $H_0$ is a nonrelativistic kinetic term

$$H_0 = \sum_{i=0}^{2} m_i + \frac{p^2}{2m_i}, \tag{2.2}$$

and the potential contains four terms:

$$V_{ij}(\vec{p}, \vec{r}) = H_{ij}^{\text{conf}} + H_{ij}^{\text{hyp}} + H_{ij}^{\text{SO}} + H_{ij}^{\text{A}}, \tag{2.3}$$

in which $H^{\text{conf}}$ is a conventional linear plus Coulomb-like potential with running $\alpha_s$:

$$H_{ij}^{\text{conf}} = -\left(C + br - \frac{\alpha_s(r)}{r}\right)\left(-\frac{\lambda_i \lambda_j}{4}\right), \tag{2.4}$$

and $H^{\text{hyp}}$ in a conventional hyperfine splitting term

$$H_{ij}^{\text{hyp}} = \frac{\alpha_s(r)}{m_i m_j}\left\{\frac{8\pi}{3}\vec{S}_i \cdot \vec{S}_j \delta^3(r_{ij}) + \frac{1}{r_{ij}^3}\left[\frac{3\vec{S}_i \cdot \vec{r}_{ij}\vec{S}_j \cdot \vec{r}_{ij}}{r_{ij}^2} - \vec{S}_i \cdot \vec{S}_j\right]\right\}\frac{\lambda_i \lambda_j}{4}, \tag{2.5}$$

where the first term is the contact term and the second the tensor term. The spin-orbit term has the form,

$$H_{ij}^{SO} = \frac{\alpha_s(r)}{r_{ij}^3}\left(\frac{1}{m_i}+\frac{1}{m_j}\right)\left(\frac{\vec{S}_i}{m_i}+\frac{\vec{S}_j}{m_j}\right)\cdot\vec{L}_{ij}\frac{\lambda_i\lambda_j}{4}$$
$$-\frac{1}{2r_{ij}}\frac{\partial H^{conf}}{\partial r_{ij}}\left(\frac{\vec{S}_i}{m_i}+\frac{\vec{S}_j}{m_j}\right)\cdot\vec{L}_{ij}, \tag{2.6}$$

and the last term $H^A$ in (2.3) is a phenomenological quark annihilation term introduced in order to take into account the annihilation of the flavour singlet states into gluons. One also needs another phenomenological term for the $\eta$, $\eta'$ states to allow for the U(1) anomaly.

Isgur and Godfrey [20] present impressive fits using such a model claiming that all mesons "from the pion to the upsilons" can be understood. We believe this to be over-optimistic. One has to bear in mind that, although the number of free parameters is not very big (quark masses, slope parameter $b$, $\alpha$, $C$, $\Lambda$, parameters for the annihilation $H^A$ and for the anomaly, and some smearing etc. parameters related to relativistic effects), some of these are not well understood. In particular the large value of $\alpha_s(s)$ at small $s$-values (of order unity) makes the one gluon exchange picture dubious. In addition the spin-orbit term, which must be present by self consistency is much too large (by $\sim$ 10 times) when fitting the baryons. Also the signs of the annihilation terms are not well understood. With transverse gluons and no light glueball state the gluon annihilation graph should always shift the flavour singlet state down in mass, which is in the wrong direction for the $0^{-+}$, $1^{--}$, $1^{++}$ multiplets. The latter difficulty might be overcome by having one of the gluons instantaneous [23], but no reliable such calculation giving all signs of $I = 0$ and $I = 1$ mass splittings correctly has been presented (cf. the discussion in connection with Fig. 1 in the introduction). We return in Sec. 6.3 to how this problem is solved in the unitarized quark model.

### 2.3. Lattice calculations and "quenched" QCD

By discretizing QCD in Euclidean space-time on a lattice some ambitious attempts have been done, which try to calculate hadron masses directly from fundamental principles (see e.g. the review by Schierholz [24]). Essentially all calculations so far have been done in the quenched approximation, that is without fermion loops using the Wilson action. Such calculations claim a light $0^{++}$ glueball $\sim 770 \pm 40$ MeV, which is very difficult to accommodate with present data on the $\pi\pi$ S wave phase shift [25]. The glueballs of other $J^P$ are predicted heavier than 1.4 GeV, always heavier than the lightest known $q\bar{q}$ states.

For $q\bar{q}$ states the quenched lattice calculations give reasonable values for $\varrho$, $A_1$, and N masses but the $\varepsilon$ is too light ($660 \pm 50$ MeV). (The $\pi\pi$ phase shift can be understood with a broad $\varepsilon(1300)$ and narrow S(975) without the "old" $\varepsilon(700)$.) In general the quenched approximation has the failure of predicting a $I = 0$ and $I = 1$ degeneracy, which is bad for in particular $0^{++}$ and $0^{-+}$ states. Also the $\Delta$—N mass splitting seems to be too small: $(\Delta - N)/N = 0.12 \pm 0.5$ [26].

In short the $q\bar{q}$ spectroscopy on the lattice is in its infancy and it probably will take

a very long time before reasonable results including the fermion determinant from quark loops can be calculated.

In the meantime a perhaps more promising approach is to first calculate the $q\bar{q}$ potential on the lattice and then use this potential as an input to conventional $q\bar{q}$ spectroscopy (Sec. 2.2), and adding quark loops along the lines we discuss in this paper. Recent calculations by Stack and collaborators [27] using a $12^3 \times 16$ lattice in a $2^6$ array of parallel microprocessors found a potential which can be very well parametrized by a linear plus Coulomb term (see Fig. 2).

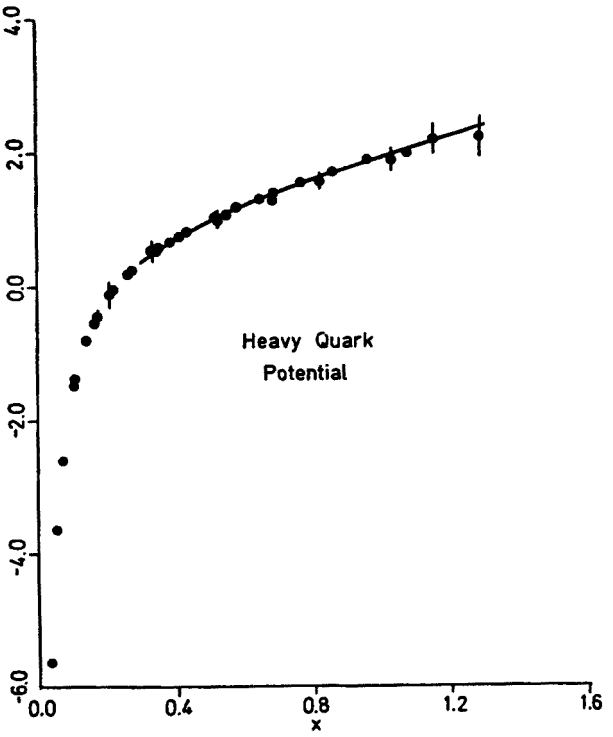


Fig. 2. The potential between two heavy coloured sources as calculated in quenched lattice QCD (Ref. [27])

$$V(r) = -\frac{\alpha_s}{r} + kr, \tag{2.7}$$

while e.g. a logarithmic potential seems excluded. Unfortunately it is not easy to extract the two parameters $\alpha_s$ and the string tension parameter $k$ from their results since the scales are not well defined without phenomenological input.

## 2.4. QCD sum rules

Much impressive theoretical work has been done on the QCD sum rules initiated by Shifman, Vainshtein and Zacharov [28–29]. For a review see Reinders lectures from last year [30]. It has much theoretical appeal since in principle it aims at predicting hadron

masses directly from the QCD Lagrangian with only a few condensate parameters and quark masses. Unfortunately this approach failed to predict the correct mass of the $\chi_b$ and is essentially limited to the first radial excitations. But, in principle quark loops are here included at least in an average sense.

The lack of a simple bridge between the QCD sum rules and the phenomenologically highly successful potential models for heavy quarkonium is disturbing. Bell and Bertlmann [31] have continued their efforts to find such a bridge and conclude that the potential which best fits the sum rule results is proportional to the fourth (!) power of $r$, and that it is flavour and mass dependent. This is in strong disagreement with conventional quarkonium models.

### *3. Perturbative fermion loops in QED and QCD*

In this section I shall discuss some rather elementary analytic properties of fermion loops in QED and QCD. Apart from the importance to understand these for their own sake, they are instructive in order to understand the behaviour of the mass shift corrections discussed later in Sections 4–5.

#### 3.1. Lepton loops in QED

Let me begin with discussing the vacuum polarization in QED using a language similar to that we use in "unitarizing the quark model". In fact I believe this is a very physical approach which is intuitively very easy to understand. It is related to the Källén-Lehmann representation of 2-point functions. We first calculate the width of a virtual photon to a lepton pair using standard techniques,

$$\Gamma/\sqrt{s} = \frac{1}{2s}\frac{1}{(2\pi)^2}\int dR_2 \bar{\Sigma}|M|^2, \tag{3.1}$$

where

$$\bar{\Sigma}|M|^2 = \tfrac{1}{3}e^2 4L^{\mu}_{\mu}(p_1, p_2) = \frac{4e^2}{3}s\left(1+\frac{2m^2}{s}\right) \tag{3.2}$$

in which $L_{\mu\nu}$ is the lepton tensor

$$4L_{\mu\nu}(p_1, p_2) = \mathrm{Tr}\,[(-\not{p}_1+m_1)\gamma_\mu(\not{p}_2+m_2)\gamma_\nu] \tag{3.3}$$

and $R_2$ two-body phase space

$$R_2 = \frac{\pi}{2}\frac{k}{\sqrt{s}} = \frac{\pi}{2}\sqrt{1-\frac{4m^2}{s}}. \tag{3.4}$$

Then

$$\frac{\Gamma}{\sqrt{s}} = \frac{\alpha}{3\pi}\frac{\pi}{2}\sqrt{1-\frac{4m^2}{s}}\left(2+\frac{4m^2}{s}\right), \tag{3.5}$$

where the $\frac{1}{3}$ comes from averaging over three initial spins. In the last factor the 2 comes from the two transverse polarizations and $4m^2/s$ from the longitudinal polarization. Let us define:

$$\operatorname{Im} \Pi(s) = -\frac{\Gamma(s)}{\sqrt{s}} = -\left(1+\frac{4m^2}{s}\right)\sqrt{1-\frac{4m^2}{s}}, \tag{3.6a}$$

$$\operatorname{Re} \Pi(s) = \frac{1}{\pi}\, s \int \frac{\operatorname{Im} \Pi(s)}{s'(s-s')}\, ds' + \Pi(0), \tag{3.6b}$$

and a photon "running mass":

$$m_\gamma^2(s) = s\Pi(s) = s \operatorname{Re} \Pi(s) - i\Gamma\sqrt{s}, \tag{3.7}$$

which vanishes for $s = 0$ (by construction) as it should in order to maintain gauge invariance. Conventionally one generally instead of a running photon mass absorbes the $s$ dependence into a running coupling constant $\alpha(s)$. That is we can sum the fermion loops in the photon propagator (Fig. 3) by renormalizing $\alpha$:

$$\frac{\alpha_0}{s} \to \frac{\alpha_0}{s - m_\gamma^2(s)} = \frac{\alpha(s)}{s}, \tag{3.8}$$

where

$$\alpha(s) = \frac{\alpha_0}{1 - \frac{\alpha}{3}\Pi(s)}. \tag{3.9}$$

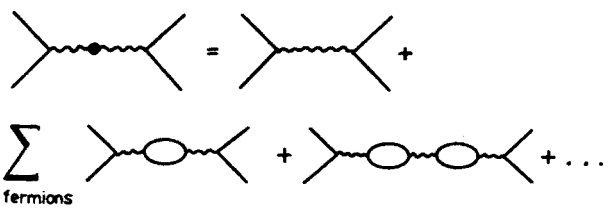


Fig. 3. The renormalized photon propagator obtained from summing graphs with charged fermion loops

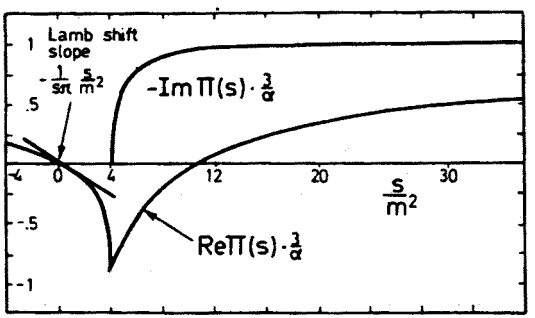


Fig. 4. The QED vacuum polarisation function (cf. Eqs. (3.6)–(3.7) and (3.10)) as a function of $s/m^2$

It is instructive to look at a plot of the function $\Pi(s)$ (Fig. 4). Its imaginary part is proportional to the phase space modified near threshold by the piece from the longitudinally polarized photon. The real part vanishes at $s = 0$ ($\Pi(0)$ is absorbed into $\alpha_0$ by renormalization) and it has a square root like behaviour below threshold. On the other hand above threshold it is nearly linear and for large $|s|$ it approaches a logarithm. More precisely the analytic form is:

$$\operatorname{Re}\Pi(s) = \frac{1}{\pi}\left\{\tfrac{5}{3} + \frac{4m^2}{s} - \left(1+\frac{2m^2}{s}\right)\sqrt{1-\frac{4m^2}{s}}\right.$$

$$\left.\times \ln\frac{1+\sqrt{1-4m^2/s}}{1-\sqrt{1-4m^2/s}}\right\}, \tag{3.10}$$

for $s > 4m^2$ and $s < 0$, while for $0 < s < 4m^2$ replace the logarithm by

$$\operatorname{arctg}\sqrt{4m^2/s-1}\,.$$

For large $|s|$ $\operatorname{Re}\Pi(s)$ has the often quoted logarithmic behaviour:

$$\operatorname{Re}\Pi(s) \approx \frac{1}{\pi}\ln(s/m^2), \tag{3.11}$$

while for very small $|s|$

$$\operatorname{Re}\Pi(s) \approx -\frac{1}{5\pi}\frac{s}{m^2}\,. \tag{3.12}$$

This small $s$ limit is relevant for the QED correction to the Lamb shift and is found in any text book on QED.

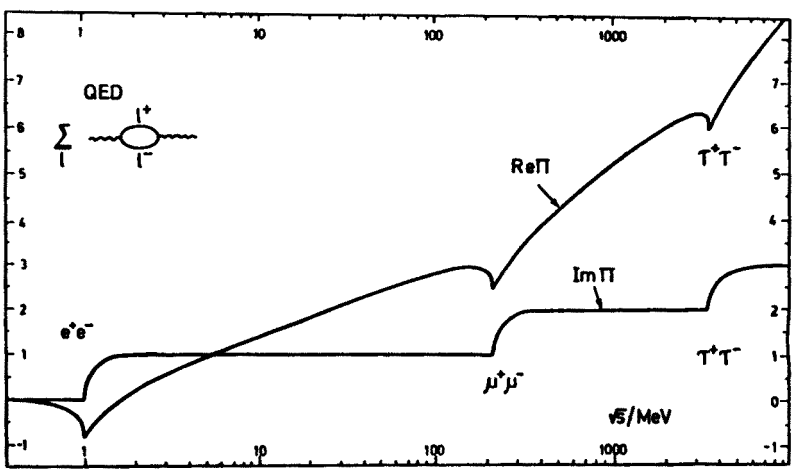


Fig. 5a

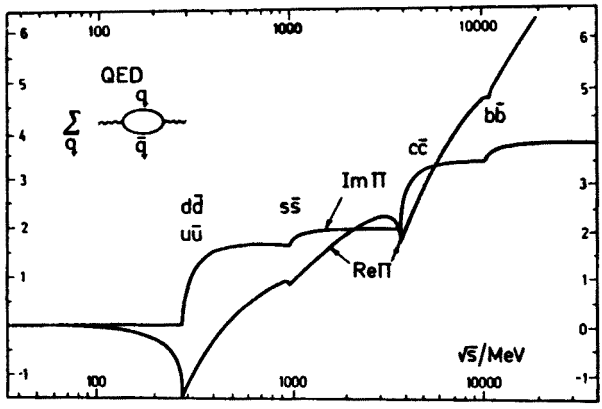


Fig. 5b

Fig. 5. The QED vacuum polarisation function taking into account (a) the $e^+e^-$, $\mu^+\mu^-$ and $\tau^+\tau^-$ thresholds, (b) the $u\bar{u}$, $d\bar{d}$, $s\bar{s}$ and $c\bar{c}$ thresholds (using the first OZI allowed threshold as threshold value)

For our purpose it is rather the behaviour near $s = 4m^2$, with the pronounced cusp, which is the most interesting. The same behaviour appears in S-wave hadron loops (for higher partial waves the cusp is smeared out somewhat).

With several thresholds there will obviously be one cusp for every threshold as shown in Fig. 5a for the $e^+e^-$, $\mu^+\mu^-$ and $\tau^+\tau^-$ thresholds. If we consider the quark thresholds we get the curves of Fig. 5b, and thus the QED $\Pi(s)$ function is a sum of Fig. 5a and 5b. There is an ambiguity as to what quark masses one should use, since really each quark threshold should be replaced by a sum over many hadron thresholds. As effective quark masses "constituent quark masses" are perhaps the best choice.

### 3.2. Quark loops in QCD

In QCD the perturbative quark loops are quite similar to those in QED apart from a color factor, a larger $\alpha_s$ and different couplings to quark flavours.

In Fig. 6 the quark loop contribution to $\Pi(s)$ is plotted (normalized such that each threshold increases $\operatorname{Im}\Pi(\infty)$ by one unit). The exact position of the thresholds are not well defined (in Fig. 6 we used the first OZI allowed threshold), since it is not clear what quark masses should be used. Really each quark threshold should because of confinement be replaced by a sum over many hadron thresholds. Such "hadronization" involves non-perturbative effects, which, however, should be small if one is far from the threshold regions.

In addition to quark loops the gluon loops contribute a piece of opposite sign to $\Pi(s)$, which reverses the sign of $\operatorname{Re}\Pi(s)$ and makes the theory asymptotically free. For $s \gg m^2$ one finds the usual expression:

$$\Pi(s) = -\frac{1}{4\pi}(11-\tfrac{2}{3}n_f)\log\frac{s}{m^2} = -\beta_0 \ln\frac{s}{m^2}, \tag{3.13}$$

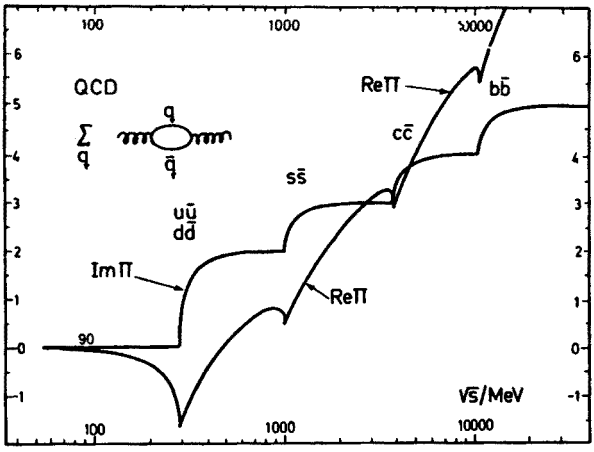


Fig. 6. The quark contribution to the QCD vacuum polarization function (using the first OZI allowed threshold as threshold value)

where $n_f$ is the number of flavours. Thus one gets the well known running $\alpha_s$:

$$\alpha_s(s) = \frac{\alpha_s}{1+\alpha_s\beta_0 \ln \frac{s}{m^2}} = \left(\beta_0 \ln \frac{s}{\Lambda^2}\right)^{-1}, \tag{3.14}$$

where

$$\Lambda^2 = m^2 \exp\left(-\frac{1}{\alpha_s\beta_0}\right).$$

By using the running $\alpha_s$ in the one-gluon exchange potential (cf. Fig. 7 and Ref. [32]) one includes perturbative quark loops corresponding to rather distant ($t$-channel) singularities.

Much more important are the nearby $s$-channel singularities (cf. Fig. 8a, b) where the quarks can recombine to form physical hadrons in the $s$-channel. Such singularities are not included, even in an average sense, by a running $\alpha_s$ in the Coulomb potential. We refer to these as nonperturbative quark loops. To calculate them we need a model for hadron three point functions. Such models necessarily involve hadron wave functions or form factors, and we must invoke some amount of phenomenology. Fortunately most of the phenomenology we need is fairly standard, and for hadronic vertices the $^3P_0$ model has been successfully shown to work for numerous hadronic decays.

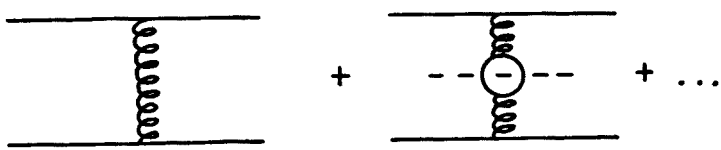

Fig. 7. The perturbative quark loops modifying the one gluon exchange potential through a running $\alpha_s(t)$

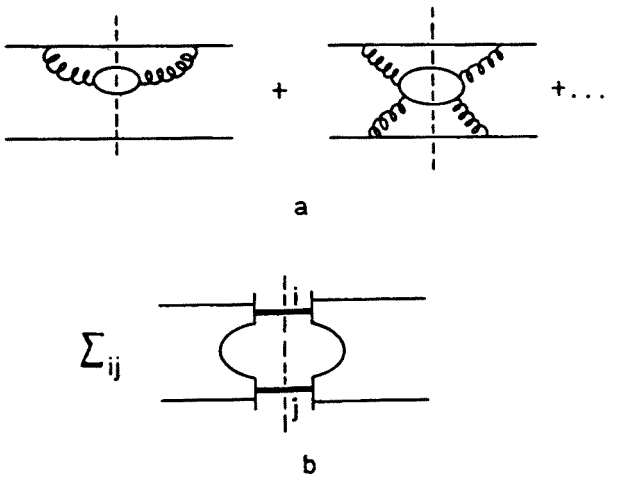


Fig. 8. Diagrams containing $s$-channel quark loops (a) which when summed, including nonperturbative contributions, contribute to the $s$-channel cuts described by intermediate two body (or multibody) hadron states (b)

### 4. *Hadron widths and the $^3P_0$ model*

As a first step in order to develop a unitarized quark model including the nonperturbative quark loops of Fig. 8 we need a model for hadronic three-point functions to be used as an input in the dispersion relations.

We use the $^3P_0$ model which includes most conventional internal symmetry relations and which has successfully been applied to various hadronic decays. It originated from some early intuitive ideas [33, 34] on quark pair creation (Fig. 9). A hadron decay is assumed to proceed in a two-step process. The creation of a quark pair in a $^3P_0$ state and with vacuum quantum numbers is followed by a rearrangement of quarks to final hadrons. In particular the Orsay group [35] have developed this model into its present form.

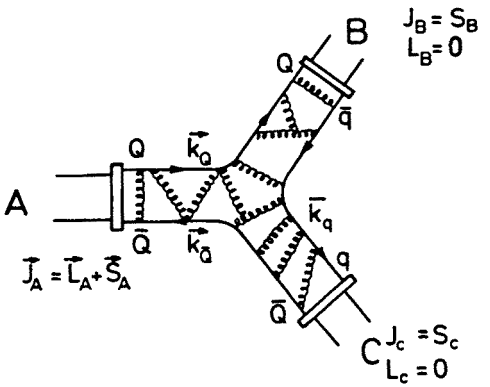


Fig. 9. Hadron three-point function described by a quark pair creation in a $^3P_0$ state and vacuum quantum numbers followed by a rearrangement of quarks into final mesons

For quarkonium this model factorizes into a flavour factor, $F_{ABC}$, a spin-angular-momentum factor $S^{-m}_{ABC}$, and a spatial overlap, $I_m$, multiplied by an overall constant the quark pair creation strength parameter $\gamma_{QPC} \approx 3.3$ as given by the formula

$$\langle BC|T|A\rangle = \gamma_{QPC} \sum_m \langle 11, m-m|00\rangle$$

$$F_{ABC} S^{-m}_{ABC} I_m(ABC), \tag{4.1}$$

where $\langle 1\,1, m\,-m|0\,0\rangle$ is a Clebsch-Gordan coefficient for coupling the P-wave of the pair to the quark spin triplet.

## 4.1. The spatial overlap $I_m$

The spatial overlap $I_m$ is given by the overlap between three $q\bar{q}$ wave functions of the hadrons involved and a function $\mathcal{Y}^m_1 = \vec{\varepsilon}_m \cdot \vec{k}\sqrt{3/4\pi}$ describing the P-wave $q\bar{q}$ pair:

$$I_m(ABC) = \tfrac{1}{8}\int d\vec{q}\,\mathcal{Y}^m_1(\vec{k}_B - \vec{q}) \times \psi_A(\vec{k}_B + \vec{q})\psi_B(-\vec{q})\psi_C(\vec{q}). \tag{4.2}$$

This overlap has the nice features that for a pointlike particle $B$ (or $C$) it reduces to conventional particle emission models including a "recoil term" (cf. Ref. [36]). It also automatically avoids double counting. For our purpose one obvious but important feature is that it gives an exponential cutoff for large decay momenta $k_B$. This is related to the finite size of hadrons as described by the wave function $\psi_A$ etc., and will ensure that any hadronic mass renormalization from a given channel is finite.

It is also instructive to note that in the special case when the decay products $B$ and $C$ are much larger than the decaying hadron $A$, the overlap is simply:

$$I_m(ABC) \propto \vec{\varepsilon}_m \cdot \vec{k}_B \psi_A(\vec{k}_B), \tag{4.3}$$

i.e. it is given only by the wave function of the decaying hadron multiplied by the $\mathcal{Y}^m_1$ factor.

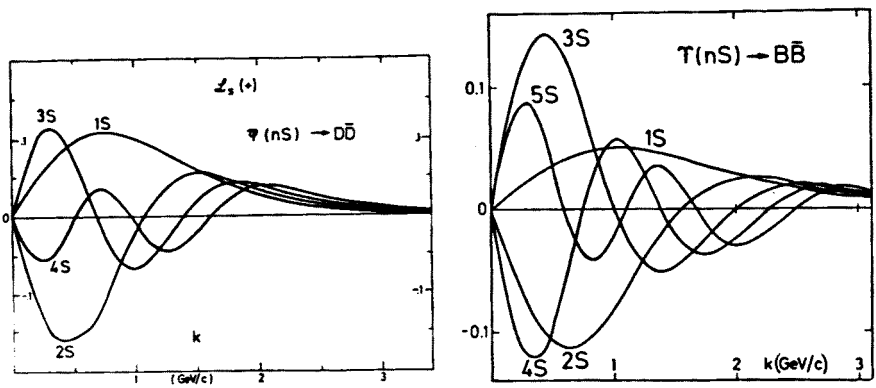


Fig. 10a,b

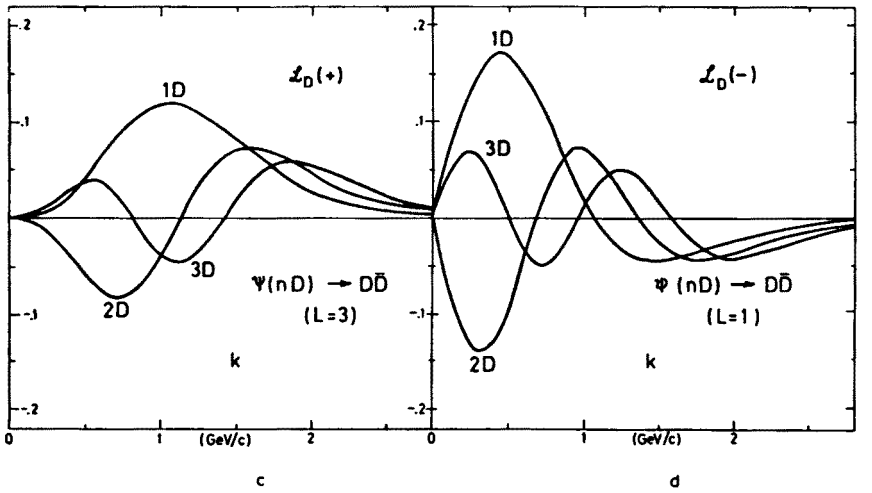


Fig. 10. Some examples of the spatial overlaps: (a) Ψ(ns) $D\bar{D}$ P-wave decay, (b) Υ(nS) $B\bar{B}$ P-wave decay, (c) Ψ(nD) $D\bar{D}$ F-wave decay, (d) Ψ(nD) $D\bar{D}$ P-wave decay

This is not an unreasonable approximation for heavy quarkonium decay like Υ(NS) → $B\bar{B}$, since the $b\bar{b}$ bound states are smaller than the $b\bar{u}$, $b\bar{d}$, $b\bar{s}$ states. In Fig. 10 we give a few examples of the spatial overlaps in the case of charmonium.

## 4.2. The spin-angular-momentum overlap

This factor is obtained by recoupling the spins and angular-momentum of the quarks in meson $A$ and the $^3P_0$ $q\bar{q}$ pair to form instead the two final mesons ($B$ and $C$) of definite spins and parity. It is straightforward to show that this recoupling can be expressed in terms of 9-$j$ symbols and some Clebsch-Gordan coefficients. One finds that the reduced widths to pseudoscalar (P) or vector mesons (V) are proportional to

$$S^2_{ABC} \propto \langle L_A 0, 10 | L 0 \rangle^2 \cdot \frac{3(2L_A+1)}{(2L+1)}$$

$$\times \sum_{S_T} \begin{bmatrix} \frac{1}{2} & \frac{1}{2} & S_B \\ \frac{1}{2} & \frac{1}{2} & S_C \\ S_A & 1 & S_T \end{bmatrix}^2 \begin{bmatrix} L_A & 1 & L \\ S_A & 1 & S_T \\ J_A & 0 & J_A \end{bmatrix}^2, \tag{4.4}$$

where the notation is defined in Fig. 9 and $S_T$ is the total spin of the four final quarks[1]. In Table I we have listed the weights as given by Eq. (4.4) (normalized such that their sum is 12). That is if everything else is identical the widths are proportional to these numbers.

For corresponding spin factors in the case of ground state and P-wave baryons see Refs [16] and [18].

[1] The symbols in Eq. (4.4) differ from conventional 9-$j$ symbols in their normalization. See e.g. Ref. [13].

TABLE I

The relative spin angular momentum weights of reduced widths to pseudosecular or vector mesons for the lowest $J^{PC}$ states of decaying particle

| $J^{CP}$ | $l$ | PP | $P\bar{V}+V\bar{P}$ | VV | SUM |
|---|---|---|---|---|---|
| $0^{-+}$ | 1 | 0 | 6 | 6 | 12 |
| $1^{--}$ | 1 | 1 | 4 | 7 | 12 |
| $0^{++}$ | 0 | 3 | 0 | 1 | 12 |
| | 2 | 0 | 0 | 8 | |
| $1^{++}$ | 0 | 0 | 4 | 0 | 12 |
| | 2 | 0 | 2 | 6 | |
| $1^{+-}$ | 0 | 0 | 2 | 2 | 12 |
| | 2 | 0 | 4 | 4 | |
| $2^{++}$ | 0 | 0 | 0 | 4 | 12 |
| | 2 | 1.2 | 3.6 | 3.2 | |

## 4.3. The flavour factor

The flavour factor $F_{ABC}$ contain the flavour symmetry, OZI rule etc. constraints. For mesons it is convenient to use matrix notation and define the $q\bar{q}$ quark content through flavour matrices $\Delta$

$$|M_a\rangle = \sum_{ij} (\Delta_a)_{ij} |q_i \bar{q}_j\rangle, \tag{4.5}$$

where $a$ in the flavour index. As usual we define:

$$\Delta = \begin{bmatrix} u\bar{u} & \pi^+ & K^+ & \bar{D}^0 & \dots \\ \pi^- & d\bar{d} & K^0 & \bar{D}^- & \dots \\ K^- & \bar{K}^0 & s\bar{s} & \bar{F} & \dots \\ D^0 & D^+ & \bar{F} & c\bar{c} & \dots \\ \vdots & \vdots & \vdots & \vdots & \end{bmatrix}. \tag{4.6}$$

The physical flavourless states are generally mixtures of the "diagonal" states:

$$\Delta_a^{\text{phys}} = \sum_i \alpha_{ai} \Delta_{ii}, \tag{4.7}$$

where the mixing matrix $\alpha$ is determined by the dynamics. For bound states $\alpha$ is a real orthogonal (energy dependent) matrix, while for finite width resonances it is in general a complex nonunitary matrix, which can be normalized to satisfy $\alpha\tilde{\alpha} = 1$.

It is often more convenient to define the mixing matrix with respect to states of pure isospin or SU3 quantum numbers:

$$\Delta_{I=1} = (u\bar{u}-d\bar{d})/\sqrt{2}, \tag{4.8a}$$

$$\Delta_{I=0} = (u\bar{u}+d\bar{d})/\sqrt{2}, c\bar{c}, \ldots, \tag{4.8b}$$

$$\Delta_1^{SU3} = (u\bar{u}+d\bar{d}+s\bar{s})/\sqrt{3}, \tag{4.8c}$$

$$\Delta_8^{SU3} = -(u\bar{u}+d\bar{d}-2s\bar{s})/\sqrt{6}. \tag{4.8d}$$

The $\Delta$ matrices are normalized such that

$$\mathrm{Tr}\,(\Delta_a \Delta_a^+) = 1. \tag{4.9}$$

For three flavours and neglecting isospin breaking the mixing matrix $\alpha$ can be parametrized by one mixing angle which is denoted $\theta$ (for pure SU3 reference states) or $\delta$ (for ideally mixed reference states). Explicitly, with the pseudoscalars and vector mesons as examples, we define:

$$\begin{pmatrix}\eta'\\ \eta\end{pmatrix} = R(\theta_P \approx 79°)\begin{pmatrix}\text{octet}\\ \text{singlet}\end{pmatrix} = R(\delta_P \approx 44°)\begin{pmatrix}s\bar{s}\\ (u\bar{u}+d\bar{d})/\sqrt{2}\end{pmatrix}, \tag{4.10a}$$

$$\begin{pmatrix}\phi\\ \omega\end{pmatrix} = R(\theta_V \approx 38°)\begin{pmatrix}\text{octet}\\ \text{singlet}\end{pmatrix} = R(\delta_V \approx 3°)\begin{pmatrix}s\bar{s}\\ (u\bar{u}+d\bar{d})/\sqrt{2}\end{pmatrix}, \tag{4.10b}$$

where

$$R(\varphi) = \begin{pmatrix}\cos\varphi & \sin\varphi\\ -\sin\varphi & \cos\varphi\end{pmatrix},$$

and

$$\theta_P = \delta_P + 35.3°, \quad \theta_V = \delta_V + 35.3°.$$

Fig. 11 summarizes graphically these mixing angles and the conventions.

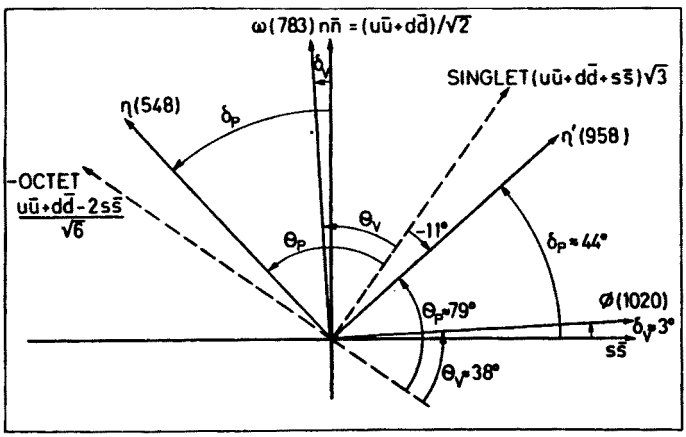


Fig. 11. The mixing of physical $\eta$ $\eta'$ and $\omega$ $\phi$ states with respect to $(u\bar{u}+d\bar{d})/\sqrt{2}$, $s\bar{s}$ and pure SU3 states

In Eq. (4.10) $\eta$, $\eta'$ and $\phi$, $\omega$ are ordered according to their masses. Conventionally one often uses the reverse order for $\eta$ and $\eta'$, whereby the mixing angles decrease by 90° ($\theta_P \approx -11°$ and $\delta_P \approx -46°$). Our convention is more natural when one wants to understand the direction of symmetry breaking (signs of mixing angles and mass splittings) through a similar dynamical mechanism for all multiplets (cf. Sec. 6).

In writing down the flavour symmetric couplings for mesons the conservation of charge conjugation also plays an important rôle. In particular the sign of

$$S = C_A C_B C_C, \tag{4.11}$$

determines whether we have symmetric ($D$-type) or antisymmetric ($F$-type) couplings. For $S = -1$ we have only one possible flavour symmetric coupling:

$$F_{ABC-} = g_- \operatorname{Tr} (\Delta_a \Delta_b^+ \Delta_c^+)_-, \tag{4.12}$$

while for $S = +1$ we have in general five different possibilities (cf. Fig. 12):

$$\begin{aligned} F_{ABC+} &= g^a \operatorname{Tr} (\Delta_a \Delta_b^+ \Delta_c^+)_+ + g^b \operatorname{Tr} (\Delta_a \Delta_b^+) \operatorname{Tr} \Delta_c^+ \\ &+ g^c \operatorname{Tr} (\Delta_a \Delta_c^+) \operatorname{Tr} \Delta_b^+ + g^d \operatorname{Tr} \Delta_a \operatorname{Tr} (\Delta_b^+ \Delta_c^+) + g^e \operatorname{Tr} \Delta_a \operatorname{Tr} \Delta_b^+ \operatorname{Tr} \Delta_c^+. \end{aligned} \tag{4.13}$$

In terms of SU3 direct products Eqs (4.12)–(4.13) correspond to the six times an octet or singlet occurs in the product:

$$(1 \oplus 8) \otimes (1 \oplus 8) \supset 8_F \oplus 8_D \oplus 8_{1 \times 8} \oplus 8_{8 \times 1} \oplus 1_{8 \times 8} \oplus 1_{1 \times 1}, \tag{4.14}$$

with obvious notation. Thus Eqs (4.12)–(4.13) are the most general charge conjugation and flavour symmetric couplings one can write down assuming only that physical mesons do not contain higher dimensions of SU3 than octets.

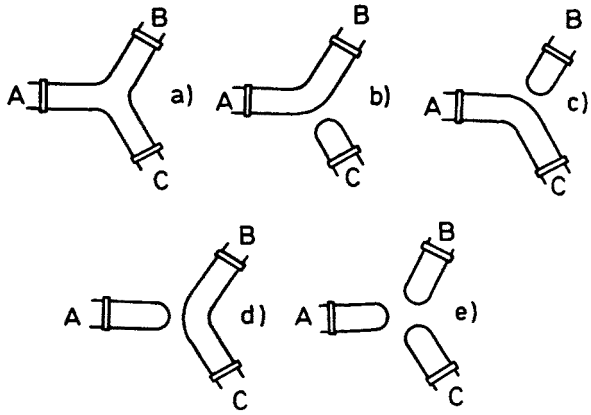


Fig. 12. The quark-line graphs corresponding to Eq. (4.13)

## 4.4. The weak OZI rule

Strictly speaking the OZI rule imposes two types of constraints on the couplings and mixing matrices $\alpha$ defined above:

(*i*) the $C$-symmetric couplings $g^b g^c g^d$ and $g^e$ vanish,

(*ii*) the mixing matrix $\alpha$ does not mix the $I = 0$ states $(u\bar{u}+d\bar{d})/\sqrt{2}$, $s\bar{s}$, $c\bar{c}$.

The second source of OZI violation (*ii*) cannot be avoided. Once the OZI rule is broken by any mechanism, and unitarity is one such mechanism, it will necessarily generate mixings of the kind (*ii*). However, the direct source of OZI violation (*i*) could be very small and all OZI breaking would be in the mass matrix, i.e. of the kind (*ii*), which would be generated through higher order diagrams. This would be similar to flavour symmetry breaking which, as well known, seems to be dominantly broken through the mass matrix.

As a working hypothesis it is thus useful to formulate a weak form of the OZI rule.

TABLE II

The flavour symmetry factor Eqs. (4.9) and (4.10a) assuming the "weak OZI rule" described in the text. Meson $A$ is assumed ideally mixed while for $B$ and $C$ the mixing is parametrised by $s_i = \sin\delta_i$, $c_i = \cos\delta_i$. The flavour quantum numbers of $B$ and $C$ are labelled by the symbols of pseudoscalar and vector mesons. Note the sum rules of Eq. (4.17)–(4.20). The light quark states of pure isospin are denoted by $I = 0$ and $I = 1$

| | $S = C_A C_B C_C = +$ | | | | $S = C_A C_B C_C = -$ | | | |
|---|---|---|---|---|---|---|---|---|
| $BC$ \ $A$ | $I=1$ | $I=0$ | $s\bar{s}$ | $c\bar{c}$ | $I=1$ | $I=0$ | $s\bar{s}$ | $c\bar{c}$ |
| $\pi^0\rho^0$ | 0 | $\sqrt{2}$ | 0 | 0 | 0 | 0 | 0 | 0 |
| $\pi^+\rho^-$ | 0 | $\sqrt{2}$ | 0 | 0 | $-\sqrt{2}$ | 0 | 0 | 0 |
| $\pi^-\rho^+$ | 0 | $\sqrt{2}$ | 0 | 0 | $+\sqrt{2}$ | 0 | 0 | 0 |
| $\pi^0\omega$ | $+\sqrt{2}c_V$ | 0 | 0 | 0 | 0 | 0 | 0 | 0 |
| $\pi\phi$ | $+\sqrt{2}s_V$ | 0 | 0 | 0 | 0 | 0 | 0 | 0 |
| $\bar{K}^0K^{*0}$ | $-\sqrt{1/2}$ | $+\sqrt{1/2}$ | 1 | 0 | $-\sqrt{1/2}$ | $\sqrt{1/2}$ | $-1$ | 0 |
| $K^0\bar{K}^{*0}$ | $-\sqrt{1/2}$ | $+\sqrt{1/2}$ | 1 | 0 | $\sqrt{1/2}$ | $-\sqrt{1/2}$ | 1 | 0 |
| $K^-K^{*+}$ | $+\sqrt{1/2}$ | $+\sqrt{1/2}$ | 1 | 0 | $\sqrt{1/2}$ | $\sqrt{1/2}$ | $-1$ | 0 |
| $K^+K^{*-}$ | $+\sqrt{1/2}$ | $+\sqrt{1/2}$ | 1 | 0 | $-\sqrt{1/2}$ | $-\sqrt{1/2}$ | 1 | 0 |
| $\eta\rho$ | $+\sqrt{2}c_P$ | 0 | 0 | 0 | 0 | 0 | 0 | 0 |
| $\eta'\rho$ | $+\sqrt{2}s_P$ | 0 | 0 | 0 | 0 | 0 | 0 | 0 |
| $\eta\omega$ | 0 | $+\sqrt{2}c_Pc_V$ | $+2s_Ps_V$ | 0 | 0 | 0 | 0 | 0 |
| $\eta'\omega$ | 0 | $+\sqrt{2}s_Pc_V$ | $-2c_Ps_V$ | 0 | 0 | 0 | 0 | 0 |
| $\eta\varphi$ | 0 | $+\sqrt{2}c_Ps_V$ | $-2s_Pc_V$ | 0 | 0 | 0 | 0 | 0 |
| $\eta'\varphi$ | 0 | $+\sqrt{2}s_Ps_V$ | $+2c_Ps_V$ | 0 | 0 | 0 | 0 | 0 |
| $D^0\bar{D}^{*0}$ | $+\sqrt{1/2}$ | $+\sqrt{1/2}$ | 0 | 1 | $\sqrt{1/2}$ | $\sqrt{1/2}$ | 0 | $-1$ |
| $\bar{D}^0D^{*0}$ | $+\sqrt{1/2}$ | $+\sqrt{1/2}$ | 0 | 1 | $-\sqrt{1/2}$ | $-\sqrt{1/2}$ | 0 | 1 |
| $D^+D^{*-}$ | $-\sqrt{1/2}$ | $+\sqrt{1/2}$ | 0 | 1 | $-\sqrt{1/2}$ | $\sqrt{1/2}$ | 0 | $-1$ |
| $D^-D^{*-}$ | $-\sqrt{1/2}$ | $+\sqrt{1/2}$ | 0 | 1 | $\sqrt{1/2}$ | $-\sqrt{1/2}$ | 0 | 1 |
| $F^+F^{*-}$ | 0 | 0 | 1 | 1 | 0 | 0 | 1 | $-1$ |
| $F^-F^{*+}$ | 0 | 0 | 1 | 1 | 0 | 0 | $-1$ | 1 |
| $\eta_c\Psi$ | 0 | 0 | 0 | 2 | 0 | 0 | 0 | 0 |

*The weak OZI rule*: (4.15)

All the breaking of the OZI rule is in the hadron mass matrix.

In other words the weak OZI rule assumes that any violation of the OZI rule can be expressed in terms of the mixing matrix $\alpha$. Clearly gluonic intermediate states can generate disconnected quark line diagrams which would violate this rule, but those may be small insofar as they cannot be included in the mixing matrix $\alpha$. To test this weak OZI rule model-independently is not a simple matter. First, we must determine the mixing matrix $\alpha$ (from e.g. radiative decays) and then test whether the first term in Eq. (4.13) reproduces the observed branching ratios of hadronic decays, assuming that SU3 violations are negligible (or can be corrected for).

In general we assume the weak OZI rule to be a sufficiently good approximation i.e. we use Eq. (4.13) with only $g^{(a)}$ different from zero. For the tensor mesons [11, 37, 38] there are some indications that this approximation fails, but even there it is difficult to disentangle this effect from SU3 breaking which also is present.

In Table II we list the flavour factors, for 4 flavours, obtained from

$$(F_{ABC})_{\pm} = \mathrm{Tr}\,(\Delta_a \Delta_b^{+} \Delta_c^{+})_{\pm}, \tag{4.16}$$

in a reference frame where $A$ is ideally mixed and the mixing of $B$ and $C$ parametrized by the mixing angle $\delta$ defined above in Eq. (4.10).

## 4.5. Completeness relations

When one sums over a complete set of $SU6_W$ related intermediate states, neglecting phase space and spatial overlap differences, one finds certain useful completeness relations or sum rules. E.g. summing over all PP, PV or VV thresholds one gets equal contributions to all octet states, only the octet–singlet degeneracy may be split. To maintain also octet–singlet degeneracy in the output, thresholds of opposite charge conjugation (i.e. opposite sign $S = C_A C_B C_C$) must contribute with equal weights.

The flavour symmetry gives the following contributions using Table II. For $S = +$

$$\sum_{BC} F_{ABC+} F_{ABC+} = \begin{pmatrix} 6 & 0 & 0 & 0 \\ 0 & 10 & 2\sqrt{2} & 0 \\ 0 & 2\sqrt{2} & 8 & 0 \\ 0 & 0 & 0 & 0 \end{pmatrix} + \begin{pmatrix} 2 & 0 & 0 & 0 \\ 0 & 2 & 0 & 2\sqrt{2} \\ 0 & 0 & 2 & 2 \\ 0 & 2\sqrt{2} & 2 & 10 \end{pmatrix}, \tag{4.17}$$

and for $S = -$

$$\sum_{BC} F_{ABC-} F_{ABC-} = \underbrace{\begin{pmatrix} 6 & 0 & 0 & 0 \\ 0 & 2 & -2\sqrt{2} & 0 \\ 0 & -2\sqrt{2} & 4 & 0 \\ 0 & 0 & 0 & 0 \end{pmatrix}}_{\text{noncharm}} + \underbrace{\begin{pmatrix} 2 & 0 & 0 & 0 \\ 0 & 2 & 0 & -2\sqrt{2} \\ 0 & 0 & 2 & -2 \\ 0 & -2\sqrt{2} & -2 & 6 \end{pmatrix}}_{\text{charm}}, \tag{4.18}$$

where the states are those in the ideal frame ($I = 1$, $I = 0$, $s\bar{s}$, $c\bar{c}$) and where we have separated the contributions from the charm quark in the second matrix. As easily seen by summing Eqs (4.17) and (4.18) one obtains the unit matrix times $4N_f$. By transforming Eqs. (4.17)–(4.18) to the frame of pure SU3 states the $3 \times 3$ submatrix is always diagonal being

$$\begin{pmatrix} 6 & 0 & 0 \\ 0 & 6 & 0 \\ 0 & 0 & 12 \end{pmatrix} \quad \text{for} \quad S = +, \quad \text{and} \quad \begin{pmatrix} 6 & 0 & 0 \\ 0 & 6 & 0 \\ 0 & 0 & 0 \end{pmatrix} \quad \text{for} \quad S = -, \qquad (4.19)-(4.20)$$

where the states are ordered such that first comes the two octet states then the singlet states. Thus for $F$-type couplings the singlet decouples and is not shifted in mass, while for $D$-type couplings the singlet is shifted twice as much as the octet. The same results hold for any $SUN_{flavour}$, i.e. for just isospin (neglecting $s\bar{s}$, $c\bar{c}$ etc.) the $I = 0$ decouples (by $G$-parity) for $S = -$, but for $S = +$ it is shifted twice as much as the $I = 1$ state.

For the spin-angular momentum part similar completeness relations hold. Thus from the properties of the 9-$j$ symbols we have:

$$\sum_{S_B S_C} \begin{bmatrix} \frac{1}{2} & \frac{1}{2} & S_B \\ \frac{1}{2} & \frac{1}{2} & S_C \\ S_A & 1 & S_T \end{bmatrix}^2 = 1, \qquad (4.21)$$

and

$$\sum_{L, S_T} \langle L_A 0, 10 | L 0 \rangle \frac{3(2L_A+1)}{(2L+1)} \begin{bmatrix} L_A & 1 & L \\ S_A & 0 & S_T \\ J_A & 0 & J_A \end{bmatrix}^2 = 1. \qquad (4.22)$$

Thus summing over all PP, PV and VV thresholds, again neglecting the spatial overlap and phase space, all octet states are shifted equally. In Table I the sum rules Eqs. (4.21)–(4.22) result in the same number (12) of the last column.

## 4.6. Comparison of the $^3P_0$ model with experiment

The $^3P_0$ model can most directly be tested by comparing with a large number of different mesonic and baryonic decays. Various authors [39–41] have performed such tests and found that with $\gamma_{QPC} \approx 3.4$ and harmonic oscillator wave functions one can reproduce a large number of known experimental widths, including $\varrho \to \pi\pi$, radial excitations of psions and upsilons (cf. Fig. 13) and various baryon decay widths. Although there

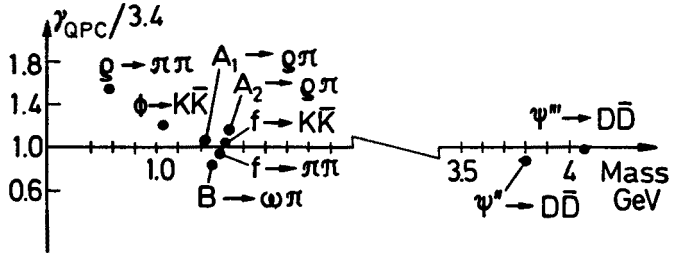


Fig. 13. Determination of $\gamma_{QPC}$ using various experimental widths [37]

are a few experimental widths, which are off by up to a factor of two the over all agreement is impressive. In fact, one should of course expect deviations since (*i*) $SU6_W$ (although more restrictive than the $^3P_0$ relations) is sometimes broken by up to 50% (*ii*) the hadronic wave functions are uncertain and (*iii*) relativistic corrections are sometimes large.

But, with these reservations the $^3P_0$ model is a good over all model for hadronic decays and we can with some confidence use it as an input to the unitarization described in the following sections.

## *5. The unitarization of the quark model and nonperturbative quark loops*

### 5.1. Non-relativistic coupled channel model

In the nonrelativistic limit the unitarization can most easily be formulated using a multichannel Schrödinger equation. In fact the formalism can be looked upon as a generalization of the over 50 years old work of Weisskopf and Wigner [42] for coupling states to the continuum.

One divides the Hilbert space into two sectors: the confined channels $|i\rangle$, which are the same as the $c\bar{c}$, $b\bar{b}$ etc. states in naive models, and the continuum channels $|k\rangle$, which are composed of two (or more) hadron states (e.g. $\pi\pi$, $K\bar{K}^*$, $D\bar{D}$ etc.). The Hamiltonian can be decomposed in the following way

$$H = \begin{pmatrix} H_0 & 0 \\ 0 & H_0^c \end{pmatrix} + \begin{pmatrix} 0 & H_{QPC} \\ H_{QPC} & 0 \end{pmatrix} \begin{matrix} \} \text{ confined channels} \\ \} \text{ continuum channels} \end{matrix} \tag{5.1}$$

Here $H_0$ is given by the usual $c\bar{c}$ or $b\bar{b}$ single channel model whose mass spectrum (= bare mass $M_i^{bare}$) and wave functions $|i\rangle$ are assumed to be known from solving the Schrödinger equation, $H_0|i\rangle = M_i^{bare}\,|i\rangle$, in the usual way. The part $H_0^c$ is assumed to contain only the kinetic energy of the two meson channels; i.e., were it not for $H_{QPC}$ no meson–meson interaction would occur, and the states $|i\rangle$ would be stable (zero width) states.

The $^3P_0$ quark pair creation Hamiltonian $H_{QPC}$ described in the previous sections and pictured by the quark line diagram of Fig. 9, where $A$ represents the confined state $|i\rangle$ and $B$ and $C$ form together the continuum states $|k\rangle$. In analogy with the Weisskopf–Wigner case, our full Hamiltonian Eq. (5.1) generates finite widths to the resonances and shifts the bare masses i.e. the eigenvalues of $H_0$ by amounts $\Delta E$; which depends on $H_{QPC}$. In addition, one finds, at the same time, the resonance mixing matrix $\alpha$ induced by $H_{QPC}$ such that the physical resonance states are mixtures between the bare confined states $|i\rangle$. Finally, the physical resonance states will mix with the continuum states $|k\rangle$, i.e., they contain a continuum component in their wave function. This continuum represents a multiquark component, similar to the "$q\bar{q}$ sea", although here always in the form of two virtual hadrons.

The actual form of $H_{QPC}$ is not very important for the unitarization. The crucial feature that we need is that $H_{QPC}$ will give energy dependent vertex functions which, due to the

finite size of the hadrons, give an automatic cut-off in the dispersion integrals. Similarly although our derivation is initially non-relativistic we show later that it can easily be thrown into a relativistic form. We suppress for simplicity many indices ($L$, $J^{PC}$, flavour, channels $BC$, etc.), which can be included in an obvious way.

Starting from the full Hamiltonian of Eq. (5.1), one can derive an effective Hamiltonian $H^{\text{eff}}$ (or a mass matrix), which describes the finite width physical resonances. For this purpose one uses as reference frame the eigenstates $|i\rangle$ of $H_0$ and the free eigenstates of $H_0^c$

$$H_0|i\rangle = M_i^{\text{bare}}|i\rangle, \tag{5.2}$$

$$H_0^c|k\rangle = E_k|k\rangle, \tag{5.3}$$

and looks for eigenstates of the full Hamiltonian of the form

$$|\psi_n\rangle = \sum_{nj} a_{nj}|j\rangle + \int dk c_n(k)\,|k\rangle dk. \tag{5.4}$$

Here the symbolic integral sign also stands for sums over the discrete variables (for example, different channels $BC$) which we have suppressed. Inserting this in the full problem:

$$H|\psi_n\rangle = M_n|\psi_n\rangle, \tag{5.5}$$

one easily finds the exact relations:

$$c_n(k) = \sum a_{ni} \frac{\langle k|H_{\text{QPC}}|i\rangle}{M_n - E_k}, \tag{5.6}$$

and

$$(H_{ni}^{\text{eff}} - M_{ni})a_{ni} = 0, \tag{5.7}$$

where

$$H_{ni}^{\text{eff}} = M_n^{\text{bare}}\delta_{ni} - \int \frac{\langle n|H_{\text{QPC}}|k\rangle\,\langle k|H_{\text{QPC}}|i\rangle}{M_n - E_k}. \tag{5.8}$$

In deriving these relations one needs only the orthogonality relations $\langle i|j\rangle = \delta_{ij}$, $\langle i|k\rangle = 0$ and $\langle i|H_{\text{QPC}}|j\rangle = 0$ and $\langle k|H_{\text{QPC}}|k'\rangle = 0$ which follow from the basic form of $H$ assumed in Eq. (5.1).

When the resonance is below all thresholds Eq. (5.8) can be used as such. Above the first threshold the resonance states are not stationary, and the integral must be interpreted as a principal value integral. It is then appropriate to add an imaginary part (Eq. (5.11) below), which describes the finite widths of decaying states.

Note that Eqs. (5.6)–(5.8) are exact, although Eq. (2.8) looks like a second order perturbation term. The integrals are all finite, since $H_{\text{QPC}}$ gives a natural cut-off due to the finite size of the hadrons, described by the $q\bar{q}$ wave functions. The second term in Eq.

(5.8) is the mass shift term and can be written:

$$\mathrm{Re}\,\Pi_{ij}(E) = -\int \frac{\langle i|H_{\mathrm{QPC}}|k\rangle\,\langle k|H_{\mathrm{QPC}}|j\rangle}{E-E_k}\,dk \tag{5.9}$$

$$= -\frac{1}{\pi}\int \frac{\langle i|H_{\mathrm{QPC}}|k\rangle\,\langle k|H_{\mathrm{QPC}}|j\rangle \varrho(k)}{E-E_k}\,dE_k, \tag{5.10}$$

where the latter form is obtained when the $k$ variable is replaced by $E_k$, whereby the phase space factor $\varrho(E)$ appears.

For the case when a continuum channel is open, one introduces an absorptive part to the effective Hamiltonian by adding an imaginary part:

$$\mathrm{Im}\,\Pi_{ij}(E) = -\langle i|H_{\mathrm{QPC}}|k\rangle\,\langle k|H_{\mathrm{QPC}}|j\rangle \varrho(E)\theta(E-E_{\mathrm{th}}), \tag{5.11}$$

whereby $\Pi_{ij}(E)$ has the proper analytic threshold behaviour containing the threshold cuts. The $\mathrm{Im}\,\Pi_{ij}$ is simply given by the widths and the $^3\mathrm{P}_0$ model. The complex mass matrix is then:

$$M_{ij}(E) = M_i^{\mathrm{bare}}\delta_{ij} + \Pi_{ij}(E). \tag{5.12}$$

## 5.2. Using unitarity and analyticity to define a more general model

At this stage it is useful to note that we can forget about the multichannel Schrödinger equation from which we started and define a more general unitarization procedure. We can consider Eq. (5.10) as a dispersion relation:

$$\mathrm{Re}\,\Pi_{ij}(E) = -\frac{1}{\pi}\int \frac{\mathrm{Im}\,\Pi_{ij}(E')}{E-E'}\,dE'. \tag{5.10'}$$

Then we can actually discard the Schrödinger equation and use analyticity and unitarity alone to define our mass matrix. Thereby we also make the formalism more general and easily modified to a relativistic form:

$$M_{ij}^2(s) = (M_i^{\mathrm{bare}})^2\delta_{ij} + \Pi_{ij}^{\mathrm{rel}}(s), \tag{5.12'}$$

$$\mathrm{Re}\,\Pi_{ij}^{\mathrm{rel}}(s) = -\frac{1}{\pi}\int \frac{\mathrm{Im}\,\Pi_{ij}^{\mathrm{rel}}(s)}{s-s'}\,ds'. \tag{5.10''}$$

For the light mesons it is clearly important to have a relativistic formulation. Of course the $^3\mathrm{P}_0$ model must be replaced by a model derived from some phenomenological Lagrangian with a cut-off, or with some educated guess of the behaviour of $\mathrm{Im}\,\Pi(s)$. The flavour symmetry factor is still applicable to the relativistic generalization, while the spin-orbital angular momentum factor can only be used as a guide to relate various coupling constants.

Below we use the relativistic notation and drop the superscript rel in $\Pi(s)$. The corresponding nonrelativistic formulas are obvious.

### 5.3. The resonance mixing matrix $\alpha$ and the hadronic mass shifts

The mass matrix is diagonalized by an $s$-dependent mixing matrix $\alpha(s)$

$$m_i^2(s) = (\alpha^{-1}(s)M^2(s)\alpha(s))_{ii}. \tag{5.13}$$

This mixing matrix can be normalized such that it is orthogonal, i.e. it satisfies $\alpha^{-1} = \alpha^{\mathrm{T}}$ and becomes complex above the first threshold. (Note that it is not unitary above this threshold.) We may for convenience normalize $\alpha$ instead such that

$$\sum_n |\alpha_{ni}|^2 = 1, \tag{5.14}$$

although above the threshold the resonances are not exactly orthogonal in the usual sense (cf. Ref. [43]). The eigenvalues $m_i^2(s)$ define the true physical masses and widths:

$$(m_i^{\mathrm{phys}})^2 = \mathrm{Re}\, m_i^2(s)|_{s=(m_i^{\mathrm{phys}})^2}, \tag{5.15a}$$

$$m_i^{\mathrm{phys}}\Gamma_i^{\mathrm{phys}} = -\mathrm{Im}\, m_i^2(s)|_{s=(m_i^{\mathrm{phys}})^2}. \tag{5.15b}$$

This definition differs, for broad resonances, from the position of the $S$-matrix poles, i.e. the zeroes of $\det(M_{ij}^2(s)-s)$, but has the advantage that it does not depend on the analytic continuation. Therefore in principle this mass and width can be determined from data directly.

### 5.4. The continuum mixing and the overall normalization

The mixing matrix $\alpha_{ij}(s)$ determines the coefficients $a_{ni}$ in Eq. (5.4) apart from the overall normalization, $N_n$, which depends on both $a_{ni}$ and the continuum mixing $c_n(k)$

$$a_{ni} = \alpha_{ni}N_n. \tag{5.16}$$

For the continuum mixing one can derive [14] in the approximation of near diagonal $\alpha_{ni}$:

$$\int |c_n(k)|^2 dk \approx N_n^2 \frac{1}{\pi} \int_{s_{\mathrm{th}}}^{\infty} \frac{-\mathrm{Im}\, \Pi_i(s')ds'}{|m_i - im_i\Gamma_i - s'|^2}. \tag{5.17}$$

Finally the normalization condition:

$$\sum_i |a_{ni}|^2 + \int |c_n(k)|^2 dk = 1 \tag{5.18}$$

determines $N_n$:

$$N_n = \left[1 + \frac{1}{\pi} \int_{s_{\mathrm{th}}}^{\infty} \frac{\mathrm{Im}\, \Pi(s')}{|m_n^2 - im_n\Gamma_n - s'|^2}\, ds'\right]^{-1/2}. \tag{5.19}$$

## 5.5. Unitary multichannel partial wave amplitudes

Assuming only that the $T$-matrix elements are dominated by a sum of $s$-channel resonances we can write down explicitly unitary partial wave amplitudes (see Fig. 14):

$$T_{AB\to CD} = \sum_{ij} G_{ABi}(s)\,[(M_i^{\text{bare}})^2 + \Pi_{ij}(s) - s]^{-1} G_{CDj}(s), \tag{5.20}$$

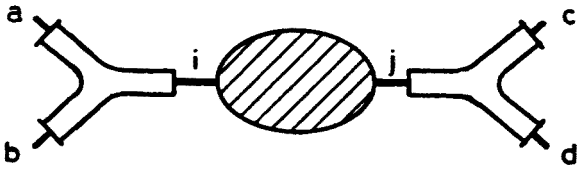


Fig. 14. Graphical representations of Eq. (5.20) where the blob in the propagator is described in Fig. 15

where the unitarity condition cf. Eq. (5.11) (see Fig. 15):

$$\text{Im}\,\Pi_{ij}(s) = -\sum_{CD} G_{CDi}(s) G_{CDj}(s), \tag{5.21}$$

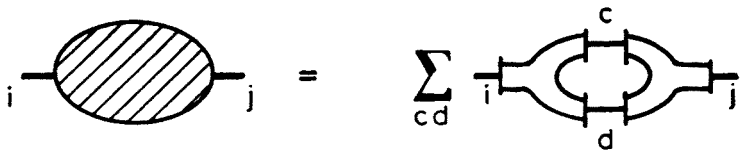


Fig. 15. The propagator as a sum over "bare" mass term and unitarity loops (cf. Eqs (5.21)–(5.23))

and the real part of $\Pi$ given by

$$\text{Re}\,\Pi_{ij}(s) = -\frac{1}{\pi} \mathcal{P} \int \frac{\text{Im}\,\Pi(s')}{s - s'}\, ds'. \tag{5.22}$$

The functions $G_{CDi}(s)$ are built from phase space and overlaps as discussed in Sec. 4 and 5.1.

$$G_{CDi}(s) = g_{CDi} \left(\frac{k_C}{\sqrt{s}}\right)^{\frac{1}{2}} k_C^l F_{iCD}(s), \tag{5.23}$$

where $g$ is a coupling constant and $F(s)$ a hadronic form factor. In the nonrelativistic approximation the product $g_{CDi} F_{iCD}(s) k_C^l$ is given by $\langle CD|T|i\rangle$ of Eq. (4.1).

For broad resonances the shape will be significantly distorted (compared to naive Breit–Wigner forms) as a result of (*i*) the $s$-dependence of $\text{Re}\,\Pi(s)$ and (*ii*) the mixing matrix $\alpha_{ji}(s)$. In particular for S-wave resonances ($\kappa$, $\varepsilon$ and $A_1$) the cusps in $\text{Re}\,\Pi(s)$ produce very distorted resonance shapes [10, 12]. Then it is crucial to compare theory and experiments with phase shifts and Argand diagrams, rather than with masses and widths.

## 5.6. The Chew-Mandelstam function $C(s)$ and the general behaviour of Re $\Pi(s)$

An illustrative and instructive example of the behaviour of Re $\Pi(s)$ near threshold is provided by a simple model where the hadronic form factor ($F_{iCD}$ in Eq. (5.23)) is put equal to one. This is of course unphysical since it implies point-like hadrons. For S-waves Im $\Pi$ is simply proportional to phase space. Then one finds a Re $\Pi(s)$ rather similar to the QED case discussed in Sec. 3.1, Eq. (3.10). The function $\Pi(s)$ is proportional to the Chew-Mandelstam function [44] (see also Ref. [45]), which may be thought of as a "complex relativistic phase space". Its imaginary part is simply phase space:

$$\text{Im } C(s) = \frac{2k}{\sqrt{s}}\,\theta(s-s_{\text{th}}) \tag{5.24}$$

with $s_{\text{th}} = (m_C+m_D)^2$ and the full function

$$C(s) = C(s, m_C^2, m_D^2) = -\frac{2}{\pi}\left\{-\frac{1}{s}[(m_C+m_D)^2-s]^{\frac{1}{2}}[(m_C-m_D)^2-s]^{\frac{1}{2}}\right.$$

$$\times \ln\left[\frac{[(m_C+m_D)^2-s]^{\frac{1}{2}}+[(m_C-m_D)^2-s]^{\frac{1}{2}}}{2(m_Cm_D)^{\frac{1}{2}}}\right]$$

$$\left.+\frac{m_C^2-m_D^2}{2s}\ln\frac{m_C}{m_D}-\frac{m_C^2+m_D^2}{2(m_C^2-m_D^2)}\ln\frac{m_C}{m_D}-\tfrac{1}{2}\right\}, \tag{5.25}$$

where a subtraction constant has been defined such that $C(0) = 0$, and where the square root and ln functions must be properly continued analytically from $s < (m_C-m_D)^2$, when $s$ is above this range. The normalization of (5.25) is such that for $F(s) = 1$ and $l = 0$

$$\Pi_{ij}(s) = -\tfrac{1}{2}\sum_{CD} g_{CDi}g_{CDj}C(s, m_C^2, m_D^2). \tag{5.26}$$

In Fig. 16 the function $C$ is displayed with the K$\pi$ threshold as an example.

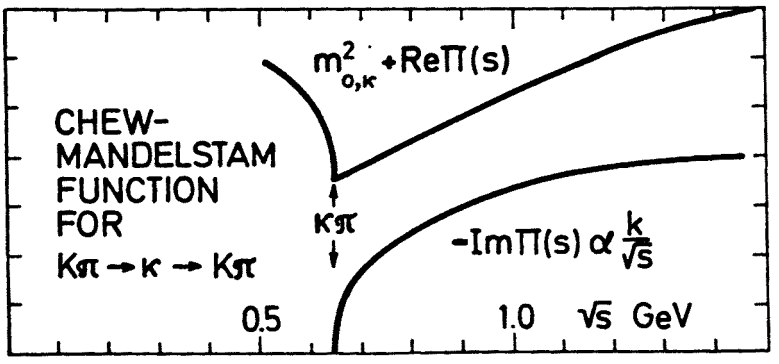


Fig. 16. The Chew-Mandelstam function with the kinematics of $\kappa \to K\pi \to \kappa$

For nonrelativistic "complex phase space" used by Flatte [46] one simply has in the equal mass case $m_C = m_D = m$:

$$C_{NR}(s) = (4m^2 - s)^{\frac{1}{2}}, \tag{5.27}$$

i.e. $\mathrm{Im}\, C_{NR} = 2k\theta(s-4m^2)$ and $\mathrm{Re}\, C_{NR} = (4m^2-s)^{1/2}\,\theta(4m^2-s)$. It differs from $C(s)$ in that instead of the near linear rise above threshold it is constant and it lacks the logarithmic asymptotic behaviour.

Of course there is always the ambiguity of subtractions and that we can add an arbitrary polynomial, if we cannot restrict the asymptotic behaviour of $\Pi(s)$. In practice for finite size hadrons the form factor $F$ always gives an effective cut off i.e. $\mathrm{Im}\,\Pi(s) \to 0$. Then no subtractions are needed and without singularities at infinity also $\mathrm{Re}\,\Pi(s)$ $\to$ constant, where the constant can be absorbed into the bare mass.

Another simple but instructive example is the function (putting $m_C = m_D = m$):

$$D(s) = [(4m^2 - s)\,(4M^2 - s)]^{\frac{1}{2}} + P(s), \tag{5.28}$$

where $P(s)$ is a polynomial. It has a finite cut at $4m^2 < s < 4M^2$, i.e. $M^2$ serves as a cut off; the "form factor" is:

$$F(s) = [(4M^2 - s)s]^{\frac{1}{2}}\theta(4M^2 - s). \tag{5.29}$$

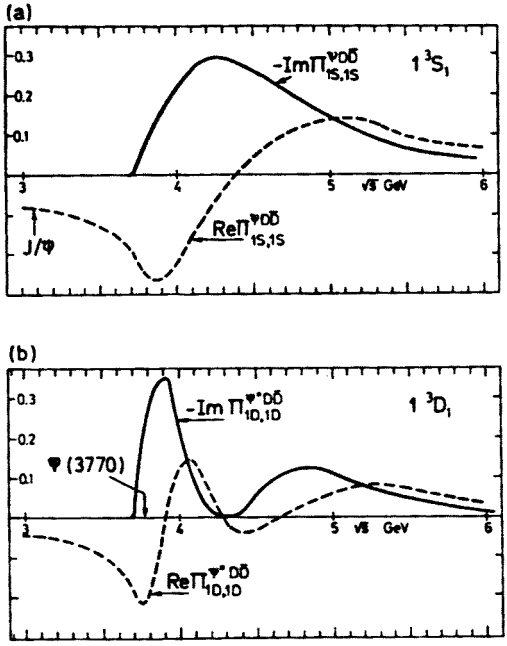


Fig. 17. Examples of the function $\Pi(s)$ for (a) $\psi(1S) \to D\bar{D}$, and (b) $\psi(1D) \to D\bar{D}$. Because of the P-wave decay the cusp is replaced by a smooth behaviour at threshold. The mass shift is given by the value of $\mathrm{Re}\,\Pi$ and the width by $\mathrm{Im}\,\Pi$ at $s = M^2_{res}$

The polynomial $P(s)$ is obtained automatically when Im $D$ is substituted into the dispersions relation (cf. Eq. (5.10)). Alternatively it can be found by the condition $D(\infty) = 0$:

$$P(s) = 2(m^2 + M^2) - s. \tag{5.30}$$

Comparing $D(s)$ with $C(s)$ one notices that they are rather similar in the threshold region. The real parts both have a square root drop before threshold and the form factor is not very important near threshold when $F(s)$ is a smooth function and the cut off sufficiently large.

Above we assumed $l = 0$. For higher partial waves the $k^{2l}$ factor makes the cusp vanish and instead there is a smooth behaviour at threshold. However, the general picture of a decreasing Re $\Pi(s)$ below threshold followed by a rise is still applicable.

For radial and orbital excitations the form factor has nodes, hence also Re $\Pi(s)$ will show oscillations. In Fig. 17 we show some examples for $c\bar{c}$ states.

### 5.7. The linearized UQM

In order to see analytically, without detailed numerical work, in what direction the mass splittings and mixing go, it is useful to study a linearized version of the UQM. This has been applied to the baryons, where the linearized model already is a rather good approximation especially for the ground state baryons [16–17]. Simply, the linearized UQM expands the $s$ dependence of $\Pi_{ij}(s)$, keeping only the constant and linear terms in $\sqrt{s}$. From Eq. (5.21)–(5.22) one finds with a cut off in $k_{\mathrm{cm}}$ approximately:

$$\Pi_{ij}(s) \approx \sum_{CD} g_{iCD} g_{jCD} [C_1 + C_2(\sqrt{s} - m_C - m_D)], \tag{5.31}$$

where the $G$'s are constants given by the flavour and spin angular momentum overlaps and $C_1$ and $C_2$ are constants. Because of completeness relations when summing over all $SU6_W$ related thresholds the $C_1$ term gives a contribution proportional to the unit matrix. (For mesons one must in addition sum over thresholds of opposite signs of $S$ in Eq. (4.11) in order to maintain singlet-octet degeneracy.) The interesting part comes from the slope parameter $C_2$ (cf. the discussion in the introduction) and the dependence on the threshold position $m_C + m_D$.

By using this linearized form and the tables of spin angular momentum factors it is easy to derive formulas relating a mass splitting such as $\Delta - N$ or $K^* - K$ to all the masses which appear in the internal loop diagram. These are discussed in more detail in Refs. [16–18] and in Secs. 6.3 and 6.5.

## *6. Comparison with experiment*

In this section we discuss the most important results of actual comparisons with data, and show how many different experimental observations can be understood as arising from quark loops within the framework of the unitarized quark model (UQM) discussed above. Most of the fits to data have been presented in much more detail in earlier work [7–18]. Only the discussion of the direction of symmetry breaking for the light mesons has not been discussed before.

## 6.1. Heavy quarkonium, $c\bar{c}$ and $b\bar{b}$ mass shifts and the upsilon (5S) mass

For heavy quarkonium the application of the UQM should be the most reliable, partly because here one has the remarkably successful "naive" potential model as a reference model, and partly because here relativistic corrections should not be too large. Thus it is natural to start the discussion with these, although the effects from quark loops here are relatively much smaller, and although historically the application started with the light mesons. Fortunately, in $b\bar{b}$ spectroscopy the upsilon (5S) mass, being just above the $B\bar{B}$ threshold turns out to be an extremely sensitive test to the underlying ideas [15].

In Fig. 18a, b we show the mass shifts for the $c\bar{c}$ and $b\bar{b}$ $n^3S_1$ ($J^{PC} = 1^{--}$) and in $P_{0,1,2}$ ($J^{PC} = 0^{++}, 1^{++}, 1^{+-}, 2^{++}$) states as a function of energy. Note the completely different relative positions of the thresholds. In $c\bar{c}$ the OZI allowed thresholds are much more spread out than in $b\bar{b}$, and in $c\bar{c}$ only two resonances are below, while for $b\bar{b}$ three resonances lie below the first threshold. This accounts for the different behaviour of the mass shifts $\Delta M$.

In general, there are several effects which contribute to the behaviour of $\Delta M$. Firstly, below the first threshold the mass shift is always negative as a result of the positivity of $-\mathrm{Im}\,\Pi_{ii}$ in Eq. (5.10), and $|\Delta M|$ increases as one approaches the threshold from below (roughly as $1/(s-s_{th})$ if the quantum numbers are the same). Above the threshold $\Delta M$ turns over to even positive values (cf. Fig. 17). Secondly, as the radial (or orbital) excitation increases the $|\Delta M|$ also usually decreases because of the node structure. Thirdly, if the resonance mixing ($\alpha$) becomes large, it of course also affects the mass shifts. For heavy quarkonium the third mentioned effect is small except for the $\psi(1D)-\psi(2S)$ mixing.

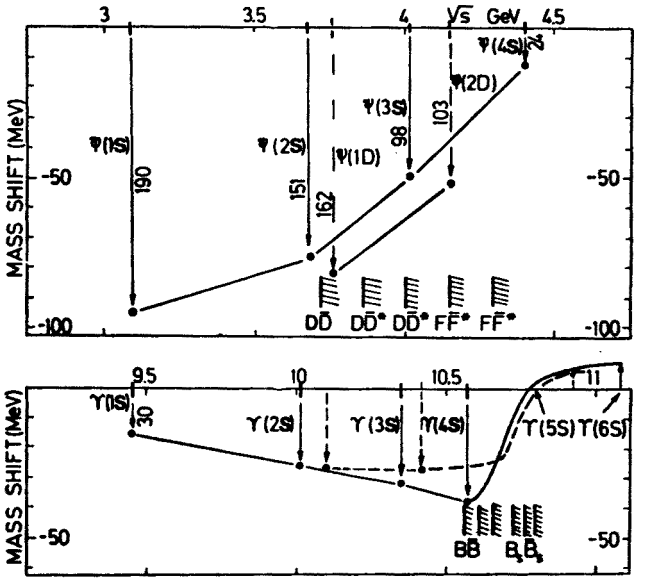


Fig. 18. The mass shifts of the S and D wave states as a function of mass for ($c\bar{c}$) states (a) and for $b\bar{b}$ states (b). The curves are shown to guide the eye. Note in particular the sharp increase in the mass shift at the opening of the $B\bar{B}$ etc. thresholds

In $c\bar{c}$ the first and second effects compete below threshold such that the second wins and shifts $\psi(1S)$ slightly more than $\psi(2S)$. For $b\bar{b}$ on the other hand, the $1/(s-s_{th})$ effect shifts the 1S much less ($-30$ MeV) than the 4S ($-74$ MeV). Above threshold $\Delta M$ increases both in $c\bar{c}$ and $b\bar{b}$, but in the latter case the effect is much more dramatic since all "ground state" thresholds are very close to each other (Fig. 18b).

This effect makes the upsilon (5S) mass a very sensitive place to test the correctness of the above results. A naive model can easily absorb the smoothly decreasing $\Delta M$ below $B\bar{B}$ into the parameters of the potential. However, then the 5S mass will be predicted to be much lighter, more precisely by about 80 MeV lighter (as obtained if one would continue the near linear part of the curve below threshold in Fig. 18b). Experimentally preliminary data from the CUSB and CLEO groups at Cornell [47, 48] support this prediction. The experimental $NS-(N-1)S$ mass splitting sequence is thus 563, 332, 217, $\approx$ 300!, $\approx$ 150. Any naive model would predict a monotonically decreasing sequence [48].

Since $SU6_W$ relations are built into the model, SU6 breaking in the output mass spectrum can arise, apart from explicit conventional SU6 breaking in the naive mass spectrum used as bare masses, only from the very small $\sim$ 50 MeV $B^*-B$ mass splitting and from different spatial overlap functions. For heavy quarkonium both these effects turn out to be very small. Therefore we get quite small contributions to the $\psi-\eta_c$, $\psi'-\eta_c'$, $\gamma-\eta_b$ etc. mass splittings [13]. A more detailed model including relativistic effects (and thereby also $SU6_W$ breaking) could well modify this result especially for $c\bar{c}$, since small $SU6_W$ breaking in the absorptive part could easily generate substantial contributions to the $\psi-\eta_c$ splitting, since the overall mass shift is nearly 200 MeV. The sum of $B\bar{B}$ etc. channels is shown in Fig. 20.

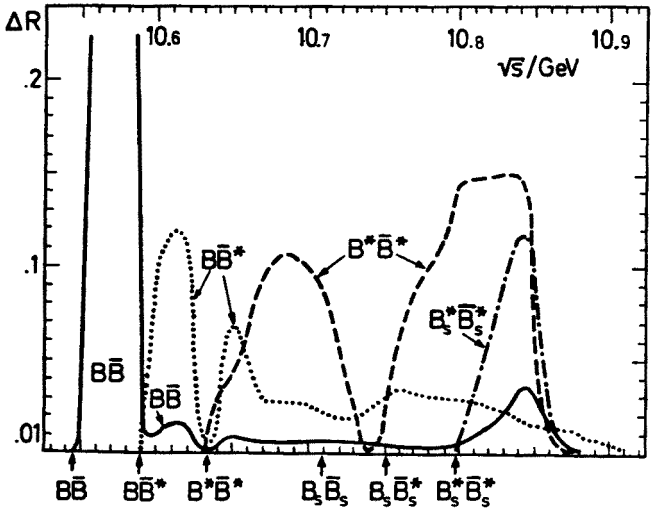


Fig. 19. The decomposition of $\Delta R$ into $B\bar{B}$ $B\bar{B}^*$ + c.c., $B^*\bar{B}^*$ and $B_s^*B_s^*$ [10]. Note that the bumps at 10.61, 10.65, 10.70 GeV do not correspond to resonances, only $\Upsilon(4S)$ and $\Upsilon(5S)$ at 10.84 GeV are present in the model. Here the mass difference of $B^*-B = B_s^*-B_s$ is assumed 42 MeV (instead of 51 MeV as in Ref. [15]). By comparing with Fig. 2b of Ref. [15] one can see the sensitivity on this mass difference

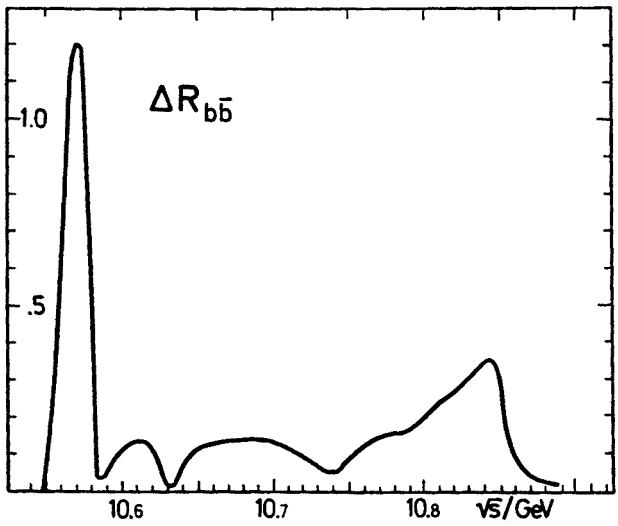


Fig. 20. The contribution to $R$ from $B\bar{B}$ etc. thresholds below 11 GeV. As in Fig. 19 $B^*-B$ is assumed here 42 MeV (not 51 MeV as in Ref. [15])

Using the formalism described in Sec. 5.5 one can also calculate $e^+e^- \to B\bar{B}$, $B\bar{B}^* + B^*\bar{B}$ and $B^*\bar{B}^*$ cross sections in a unitary frame work [15]. An important observation is then done that such cross sections have many "anomalous bumps" *not* corresponding to resonances (Fig. 19). These are rather due to the opening of new thresholds followed by dips due to nodes in the spatial overlap functions. The sum of $B\bar{B}$ etc. channels is shown in Fig. 20.

This should be a warning to anyone who would like to interpret such a structure as due to new physics e.g. hybrid states $Q\bar{Q}g$, gluonium etc. One must first exclude the possibility that the structure can be a result of the effects described above.

## 6.2. Resonance mixing, continuum mixing and radiative decays

For heavy quarkonium the resonance mixing is in general rather small i.e. the matrix $\alpha$ is near the unit matrix. However sometimes even a comparatively small mixing is important as e.g. in $e^+e^- \to 2S \to 1D$, where the direct process $e^+e^- \to 1D$ is strongly suppressed since 1D nonrelativistic wave function vanishes at the origin. We found [13] this mixing matrix element to be $0.206 + i\,0.067$. The mixing of 1D with the other $NS$ is less than 0.03 in absolute value and they do contribute a little to the 1D production. The complete mixing matrices can be found in Refs. [13–14].

Another place where small mixing is important is in M1 and E1 radiative decays. Here also the continuum mixing modifies the predictions considerably through the normalization of the states. The latter effect reduces the $c\bar{c}$ radiative widths by 20–30% and $b\bar{b}$ widths by 10–20%. On the whole these effects considerably improve the agreement with experiment, in particular the $\psi(2S) \to \chi(^3P_0)\gamma$, $\chi(^3P_2)\gamma$, $\Upsilon(2S) \to \chi_b\gamma$ and $\Upsilon(3S) \to \chi_b(2S)\gamma$ widths. There is however still some discrepancy in particular for the $\psi(2S) \to \chi(^3P_1)\gamma$ width

which is still too large since here the resonance mixing increases the width. Relativistic and gluonic effects should also modify these quantities and, although difficult to calculate reliably, they also tend to bring down the theoretical estimates. But on the whole we have a reasonable good qualitative understanding of the presently measured, radiative widths although theoretical uncertainties at the 20% level seem difficult to avoid.

### 6.3. Light quarkonium. Signs of mixing angles and mass splittings

For light quarkonium the non-relativistic model is clearly insufficient at least as far as $q\bar{q}$ wave functions are concerned. However, as long as we restrict ourselves to the ground states the detailed form of the spatial overlap or the hadronic form factor $F(s)$ in Eq. (5.23) is not very important. We can as a first step assume it to be independent of flavour quantum numbers and parametrize it by a cutoff parameter related to hadron size. Since light mesons are generally believed to be roughly of same size $\sim 0.7$ fm, it is reasonable to as a first approximation assume this cutoff to be independent of the meson in question. Then, as discussed in Sec. 5 we can construct a model which is at least formally relativistic.

Such a model is useful in order to study the direction of flavour and SU6 symmetry breaking. For the $0^{-+}$(P) and $1^{--}$(V) mesons this implies a kind of bootstrap, since the nearest thresholds (PP, PV and VV) involve the same mesons. Thus one looks for self-consistent solutions for the lightest mesons. One calculates how much is e.g. the $\varrho$ mass shifted by the $\pi\pi$, $K\bar{K}$, $\pi\varrho$, $K\bar{K}^*$, $\varrho\varrho$, ... thresholds and compares this with the corresponding shifts of the other mesons. One has a set of highly nonlinear equations and it is not simple to see what is their actual solution.

A calculation along these lines was presented already some time ago [8]. Some of the theoretical ideas are in fact quite old (see e.g. Refs. [4–6, 42, 49] and our contribution has mainly been to put all the right ingredients together and study all hadrons whithin the same framework. If one estimates e.g. only the $\varrho$ mass shift due to $\pi\pi$, it is not very useful since we do not know the bare $\varrho$ mass anyway. However if one relates this shift to other SU6 related mass shifts one can find much more interesting and reliable predictions.

Since individual mass shifts need not be small and since the weights of individual thresholds vary within large limits, it is crucial that one sums over all $SU6_W$ related thresholds. Then it is obvious that one solution to the nonlinear equations is that of exact SU6, i.e. with degenerate SU6 multiplets as input the output masses are also degenerate, although all physical masses are shifted compared to the bare masses by the same amount (cf. Sec. 4.5). With some explicit symmetry breaking such as quark mass differences or V–P "hyperfine" splitting the output spectrum is clearly not SU6 symmetric, and because of the highly nonlinear effects the actual solution can deviate substantially from the naive bare mass spectrum.

When the mass shifts are large, it may also happen that the nonlinear equations are not stable, i.e. a small perturbation from the SU6 symmetric solution is enhanced by the loop diagrams. Then the stable solution need not be SU6 symmetric, i.e. one has spontaneous symmetry breaking. In fact, our order of magnitude estimates of mass shifts indicate that this in fact could be the actual situation for the light mesons. This need not be basically

a different mechanism for the spontaneous symmetry breaking, which generally is believed to take place within QCD. It would only be a different manifestation of the same physics; the complex structure of the vacuum being phenomenologically included through the hadronic form factors. In fact, if one assumes that the nearby singularities dominate the low energy physics, and that all "low energy physics" is known from experiment, then this conclusion almost inevitably follows by self-consistency.

In the following we discuss the application of the linearized form of the UQM to the light mesons. Although it is clear that the linearization must be a very crude approximation (much cruder than for the ground state baryons), it is useful in order to see easily the direction of symmetry breaking.

Using Tables I, II it is easy to derive the following weights for the various PV and VV thresholds contributing to the pseudoscalar and vector masses:

$$\pi \propto 24\pi\varrho + 12K\bar{K}^* + 24\varrho\omega + 12K^*\bar{K}^*, \tag{6.1}$$

$$K \propto 9K^*\pi + 9K\varrho + 3K\omega + 6K\varphi + 9\eta_8 K^* + 18K^*\varrho + 6K^*\omega + 12K^*\phi, \tag{6.2}$$

$$\begin{pmatrix} \eta_{88} & \eta_{81} \\ \eta_{18} & \eta_{11} \end{pmatrix} \propto \begin{pmatrix} 36 & 0 \\ 0 & 0 \end{pmatrix} K\bar{K}^* + 12 \begin{pmatrix} 1 & -\sqrt{2} \\ -\sqrt{2} & 2 \end{pmatrix} \varrho\varrho$$

$$+4 \begin{pmatrix} 1 & -\sqrt{2} \\ -\sqrt{2} & 2 \end{pmatrix} \omega\omega + 4 \begin{pmatrix} 1 & 2\sqrt{2} \\ 2\sqrt{2} & 8 \end{pmatrix} K^*\bar{K}^* + 8 \begin{pmatrix} 2 & \sqrt{2} \\ \sqrt{2} & 1 \end{pmatrix} \varphi\varphi, \tag{6.3}$$

$$\varrho \propto 4\pi\pi + 2K\bar{K} + 8\pi\omega + 8K\bar{K}^* + \tfrac{8}{3}\eta_8\varrho + \tfrac{16}{3}\eta_1\varrho + 28\varrho\varrho + 14K^*\bar{K}^*, \tag{6.4}$$

$$K^* \propto 3K\pi + 3K\eta_8 + 6K\varrho + 6K^*\pi + 2K\omega + 4K\phi$$

$$+\tfrac{2}{3}K^*\eta_8 + \tfrac{16}{3}K^*\eta_1 + 21K^*\varrho + 7K^*\omega + 14K^*\phi, \tag{6.5}$$

where the shorthand notation should be obvious and where $K\bar{K}^*$ stands for $K\bar{K}^* + \text{c.c.}$ We do not here consider the $\omega$ and $\varphi$ because the SU3 singlet, even in the limit of degenerate thresholds, is shifted differently from the octet (cf. Sec. 4.5). Therefore for $\omega$ and $\varphi$ one would either have to include more thresholds or introduce an explicit cutoff. The weights in Eqs. (6.1)–(6.7) all add up to the same number (72) i.e., putting the P and V masses equal only a constant overall mass shift is obtained.

Using the linearized UQM these equations lead to the following relations for mass splittings and for the pseudoscalar mixing angle $\theta_P$

$$K - \pi = 3c[-5\pi + 2K + 3\eta_8 - 7\varrho - 5\omega + 6K^* + 6\varphi] + (m_s - m_u)_{\text{bare}} \tag{6.6}$$

$$(\eta + \eta')/2 - K = 3c[-3\pi - 3\eta_8 + 3\varrho + \omega + 2\varphi], \tag{6.7}$$

$$\theta_P = \tfrac{1}{2}\,\text{arc tg}\, \frac{-2\sqrt{2}\,(-6\varrho - 2\omega + 4K^* + 4\varphi) + \dfrac{\sqrt{2}}{3}\dfrac{(m_s - m_u)_{\text{bare}}}{c}}{(-9K + 6\varrho + 2\omega + 5K^* - 4\varphi) - \dfrac{(m_s - m_u)_{\text{bare}}}{12c}}, \tag{6.8}$$

where the particle name stands for its mass, $(m_s - m_u)_{bare}$ is the bare strange-nonstrange quark mass splitting and $c$ is the overall slope of the mass shift function without internal symmetry factors. Since using very general arguments $c$ is a positive number, we see that part of the $K-\pi$ splitting comes from the loops and that Eq. (6.7)–(6.8) go in the right direction compared to experiment. The ratio of (6.6) and (6.7) (where $c$ essentially cancels) is remarkably good for small $(m_s - m_u)_{bare}$. The left hand side is 1.39 and the right hand side varies between 1.34 and 1.54 when $(m_s - m_u)_{bare}$ varies between 0 and 50 MeV. With the latter value for $(m_s - m_u)_{bare}$ the mixing angle is also reasonable ($\theta = 65°$) not too far from the conventional values of 79° (quadratic mass formulas) or 66° (linear mass formulas).

For the $\varrho - \pi$ and $K^* - K$ mass splitting one similarly finds:

$$\varrho - \pi = 8c[-\pi - 2(\varrho - \omega) + \sin^2 \delta_P \eta + \cos^2 \delta_P \eta'] + \text{effect from open } \varrho \to \pi\pi, \quad (6.9)$$

$$K^* - K = -8c\sqrt{2} \sin \delta_P \cos \delta_P (\eta' - \eta) + \text{effect from open } K^* \to K\pi \text{ channel.} \quad (6.10)$$

Both these relations show that the "hyperfine" splitting $V-P$ is enhanced by the loop effects. As indicated in Eqs. (6.9)–(6.10) the fact that $\varrho \to \pi\pi$ and $K^* \to K\pi$ are open also increases these splittings. For a discussion of this open channel effect, and with a sensitive application to the upsilon states see Ref. [15].

We can roughly estimate the value of the slope parameter $c$ using $\varrho$ or $K^*$ widths (cf. the discussion in the introduction). One then finds values of $c$ in the range 0.01 to 0.03, i.e. consistent with the value 0.028 one would get from Eq. (6.7). Clearly these estimates using the linearized model should only be believed as order of magnitude estimates, since nonlinear effects are large for the light mesons.

Of special interest is, however, that such a value of $c$ is perfectly consistent with a small initial SU6 breaking. As easily seen from Eq. (6.6) a small $(m_s - m_u)_{bare}$ enhances the $K-\pi$ splitting by a factor $(1+72c)\,(m_s - m_u)_{bare}$, in the first iteration of Eq. (6.6). Summing the iterations one gets roughly $(1-72c)^{-1}(m_s - m_u)_{bare}$[1]. With $c$ in the range discussed above we have consistency with small $(m_s - m_u)_{bare}$. In fact one seems to be in the range where the spontaneous symmetry breaking discussed above becomes operative. An initially small chiral and SU6 symmetry breaking through $(m_s - m_u)_{bare}$ and hyperfine splitting, sets off in the right direction, a large symmetry breaking of the physical mass spectrum.

We conclude this subsection with one final remark already discussed in Refs. [9, 12]. This is the sign of the $I = 0$, $I = 1$ mass splitting ($\omega - \varrho$ etc.) and the angle measuring the deviation from ideal mixing $\delta$. Assuming only that the nearest group of thresholds (PP,

---

[1] More exactly, within the linearized model we can write Eqs. (6.1)–(6.5) in the form:

$$m_i = m_i^0 + c \sum_j w_{ij} m_j$$

where $w_{ij}$ are the weights discussed above. The solutions are given by the matrix $(1-cw)^{-1}$, which for sufficiently large $c$ develops a pole. This pole signals spontaneous symmetry breaking. Nonlinear effects are important for already smaller values of $c$.

or PV if parity forbids PP) determine the direction of symmetry breaking the sign is given by $S$ of Eq. (4.11):

$$\text{sign}\,(m_{I=1}-m_{I=0}) = C_A C_B C_C, \tag{6.11}$$

$$\text{sign}\,(\delta_i) = -C_A C_B C_C. \tag{6.12}$$

For the five multiplets $0^{-+}$, $1^{--}$, $1^{++}$, $1^{+-}$, $2^{++}$ this simple rule predicts 10 signs of which 9 can be tested with experiment and which all agree (cf. Sec. 2.1). The tenth sign predicts that $\delta(1^{+-})$ is negative which essentially implies [9] that the missing H′ (the $1^{+-}$ $s\bar{s}$ state) is lighter than the $1^{++}$ $s\bar{s}$ state. A similar sign rule [50] can be derived for the $Q_A - Q_B$ mixing, which is determined by whether the $K^*\pi$ or $K\varrho$ threshold is lower. Again the sign is correct. Altogether these 10 correctly predicted signs constitute considerable evidence in favour of the hypothesis that the unitarity loops are the dominant mechanism distorting the physical mass spectrum. In fact, these 10 signs, which have not been predicted correctly reliably by any other mechanism of which I am aware, constituted the main motivation and impetus for me to initially pursue this line of research and to formulate an explicit model (the UQM) with which one can make detailed comparisons with data.

### 6.4. The scalar masses and other broad resonances

The scalar mesons cannot be discussed using the linearized model of the previous subsection because the nonlinear effects, most notably the cusps related to the strong S-wave decays are very large, and in addition most states lie well above an open channel. For the same reason the Gell-Mann-Okubo mass formulas break down when applied to the scalar nonet.

Conventionally the scalar mesons are known to be problematic since they have a very anomalous behaviour, not fitting into any conventional SU3 nonet. Therefore some authors have advocated that they are 4 quark states either in a bag [51] or in the form of meson-meson "molecules" bound together by hyperfine forces [20, 52]. These suggestions either neglect the unitarity loops entirely or use a $P$-matrix framework. The latter is in principle unitary, but the way the model is formulated and interpreted physically the SU6 breaking induced by the right hand cuts is not studied systematically. For example, the model calculations presented do not include complete sums over $SU6_W$ related (open or closed) thresholds. Without such complete sums the definition of a bare mass, or in the $P$-matrix model of a "primitive" mass, becomes rather arbitrary.

The solution which we presented in Ref. [10] explains the "anomalously large" $\kappa(1350)-\delta(980)$ splitting as a result of the fact that the $\pi\eta$, $K\bar{K}$ and $\pi\eta'$ thresholds shift the $\delta$ down much more than what the $\kappa$ is shifted by the rather distant $K\pi$ and $K\eta'$ thresholds. The S(975) Clebsch to $K\bar{K}$ is the largest and the associated mass shift is also large explaining the anomalously light $s\bar{s}$ state. Both the $\delta(980)$ and the S(975) are just below the $K\bar{K}$ threshold, not because of accident, but because of the sharp drop in $\mathrm{Re}\,\Pi$ below the threshold. The large deviation of the ratio $\Gamma(\kappa)/\Gamma(\delta)$ from the SU3 value is again at least partly understood as a result of the non-Breit-Wigner shapes of these resonances, as already noted by Flatte [46] several years ago. Other broad S-wave resonances, in parti-

cular the $A_1$, should show similar deviations from naive Breit-Wigner shapes. The mixing between the isoscalar states the S and the ε becomes strongly energy dependent and complex explaining why a naive constant mass matrix, as assumed in the Gell-Mann-Okubo mass formula, is a bad approximation for the scalar mesons.

Of particular interest is that it is possible to understand the isoscalar $0^{++}$ phase shifts with $q\bar{q}$ states alone. There is no experimental evidence (see also Ref. [25]) for a light glueballs ($m \lesssim 1$ GeV) state as present lattice QCD calculations seem to require.

### 6.5. Baryon mass splittings

For the baryons the relative size of the mass splittings are smaller than in the meson case, and in the case of the ground state baryons almost all states lie below all thresholds. This makes the linearized model especially well suited for studying the ground state baryons [16].

Using the techniques described in Sec. 6.3 and a table of $^3P_0$ model internal symmetry weights, (for the ground state these are the same as $SU6_w$ weights), which were calculated and listed in Table I of Ref. [16] one can derive simple mass relations which are remarkably well satisfied. Taking only into account the meson mass splittings in the loops one finds (letting the particle name again stand for its mass):

$$\frac{\Lambda - N}{\Sigma^* - \Sigma} = \frac{\varrho - 2\pi + \frac{2}{3}\eta' + \frac{1}{3}\eta}{K^* - K + \frac{2}{3}\eta' - \frac{2}{3}\eta}, \tag{6.13}$$

$$\frac{\Sigma^* - \Lambda}{\Sigma^* - \Sigma} = \frac{1}{3}\frac{K^* - K + 2\varrho + 2\eta' - 4\pi}{K^* - K + \frac{2}{3}\eta' - \frac{2}{3}\eta}, \tag{6.14}$$

$$\frac{\Xi^* - \Xi}{\Sigma^* - \Sigma} = 1. \tag{6.15}$$

Of these the last one can also be derived from SU6 alone [53]. The left hand side of these relations are 1.54, 1.41 and 1.13 respectively, while the right hand sides 1.96, 1.64 and 1.00 respectively. By adding also the baryon mass splittings in the threshold position one finds similar relations involving also baryon masses on the right hand side, which even better agree with experiments (1.55, 1.32 and 1.00 respectively). These numbers show that it is perfectly possible that most of the baryon mass splittings (apart from effects from $(m_s - m_u)_{bare}$ and small hyperfine splitting) are induced by the unitarity loops. A more detailed fit including the nonlinear effects, imaginary parts and widths has also been done by Żenczykowski [17] with a considerable amount of success. The P-wave baryons have also been treated within the linearized model [18] with many clearly nontrivial predictions for the direction of symmetry breaking. One can also successfully relate the size of the P-wave baryon splittings to those of the ground state splittings in particular the $\Delta - N$ splitting. A more detailed analysis including the nonlinear effects and adding more thresholds, involving the P-wave baryons themselves in the loops, is in progress.

### 7. Concluding remarks

We have in these lectures discussed in some detail of how one can estimate the effects of quark loops, in particular the nonperturbative quark loops, to quarkonium masses. Traditionally 10–20 years ago, when the quark model was in its infancy, such "unitarity effects" were considered to be crucial and dominant. Today they are often neglected or "swept under the rug" hoping that they are not too large. In these lectures I have tried to convince you that such hopes are in fact unfounded, and that with the large amount of new data and theoretical input available today many, almost model independent, predictions can be made, which can be tested against experiment with remarkable success. In particular the recently discovered $\Upsilon(5S)$ turned out to be a surprisingly good place to test the underlying ideas [15], since its mass is $\sim$ 80 MeV heavier than naive models predict. Clearly if nonperturbative quark loops are important for the heavy upsilons they should be much more important for the light mesons and baryons.

In the written version of these lectures I have mainly commented on work which already have been published, adding clarifying material which was not included in the previously published papers. Only some of the most important comparisons with data are included here. Therefore the reader should consult the references [7–18] for more details on the fits to experiments.

Let me also conclude by referring to a few and by no means complete set of related work (Refs. [54–65]), which like the ones mentioned above (Refs. [4–6, 42–46]) generally agree with our philosophy. Within another context, the final state corrections to weak and electromagnetic decays, the work of Truong and collaborators [66] bare much in common with our work.

I thank my collaborators K. Heikkilä, S. Ono, M. Roos and P. Żenczykowski for many discussions on topics included in this paper. To the organizers of the 1984 Cracow School of Theoretical Physics in Zakopane I also wish to express my deep gratitude for the kind hospitality and for creating the inspiring milieu during the school.

## REFERENCES

[1] G. Zweig, in: *Development in the Quark Theory of Hadrons*, ed. D. B. Lichtenberg, S. P. Rosen, Hadronic Press, Nonantum, Mass., Vol. 1: 1974–1978, 1980 p. 22.
[2] M. Gell-Mann, *Phys. Lett.* **8**, 214 (1964).
[3] G. Zweig, *Origin of the Quark Model*, Proc. of Baryon 1980 IV Int. Conf. on Baryon Resonances, Toronto, ed. N. Isgur, University of Toronto, p. 439.
[4] G. F. Chew, *The Analytic S-Matrix*, W. A. Benjamin Inc., New York 1966.
[5] R. J. Eden, P. V. Landshoff, D. I. Olive, J. C. Polkinghorne, *The Analytic S-Matrix*, Cambridge University Press 1966; B. R. Martin, D. Morgan, G. Shaw, *Pion-Pion Interactions in Particle Physics*, Academic Press 1976.
[6] R. P. Feynman, *Photon Hadron Interactions*, W. A. Benjamin Inc., New York 1972, pp. 58, 95.
[7] N. A. Törnqvist, *Ann. Phys.* (N.Y.) **123**, 1 (1979).
[8] M. Roos, N. A. Törnqvist, *Z. Phys.* **C5**, 205 (1980).
[9] N. A. Törnqvist, *Nucl. Phys.* **B203**, 268 (1982).
[10] N. A. Törnqvist, *Phys. Rev. Lett.* **49**, 624 (1982).

[11] N. A. Törnqvist, *Phys. Rev.* **D29**, 121 (1984).
[12] N. A. Törnqvist, 7-th Int. Conf. on Experimental Meson Spectrosc. — 1983, ed. S. J. Lindenbaum, AIP, New York 1984, p. 189.
[13] K. Heikkilä, S. Ono, N. A. Törnqvist, *Phys. Rev.* **D29**, 110 (1984).
[14] S. Ono, N. A. Törnqvist, *Z. Phys.* **C23**, 59 (1984).
[15] N. A. Törnqvist, *Phys. Rev. Lett.* **53**, 878 (1984).
[16] N. A. Törnqvist, P. Żenczykowski, *Phys. Rev.* (Rapid Comm.) **D29**, 2139 (1984).
[17] P. Żenczykowski, *Z. Phys.* **C26**, 441 (1984).
[18] N. A. Törnqvist, P. Żenczykowski, Helsinki preprint HU-TFT-85-10.
[19] L. Montanet, 7-th Int. Conf. on Experimental Meson Spectroscopy-1983, ed. S. J. Lindenbaum, AIP, New York 1984, p. 479.
[20] N. Isgur, S. Godfrey, Toronto preprint, December 1983, revised February 1984.
[21] J. L. Rosner, *Quark Models*, Lectures at Advanced Studies on Techniques and Concepts of High Energy Physics, July 2–13, 1980, St. Croix V.I.
[22] C. Quigg, *Models for Hadrons*, FERMILAB-Conf.-81/78-THY, Lectures at l'Ecole d'Eté de Physique Theorique, Les Houches, Aug. 3-Sept. 11, 1981.
[23] J. F. Donogue, H. Gomm, *Phys. Lett.* **112B**, 409 (1982); *Phys. Rev.* **D21**, 1975 (1980); J. F. Donogue, Int. Conf. on Experimental Meson Spectroscopy, ed. S. J. Lindenbaum, AIP, New York 1984, p. 107.
[24] G. Schierholz, *The Hadron Spectrum in Lattice QCD*, DESY 83-129 (1984).
[25] S. R. Sharpe, M. R. Pennington, R. J. Jaffe, Harward preprint HUTP 84/A017; S. R. Sharpe, Harward preprint HUTP 84/A029.
[26] Z. Kunzt, I. Montvay, *Phys. Lett.* **139B**, 195 (1984).
[27] J. Stack, *Phys. Rev.* **D29**, 1213 (1984); E. Brooks III et al., *Phys. Rev. Lett.* **52**, 2324 (1984); S. W. Otto, J. P. Stack, *Phys. Rev. Lett.* **52**, 2328 (1984).
[28] M. A. Shifman, A. I. Vainshtein, V. I. Zacharov, *Nucl. Phys.* **B147**, 385, 448, 519 (1979).
[29] L. J. Reinders, H. R. Rubinstein, S. Yazaki, *Nucl. Phys.* **B186**, 109 (1981); **B196**, 125 (1982); **B213**, 109 (1983).
[30] L. J. Reinders, *Acta Phys. Pol.* **B15**, 329 (1984).
[31] J. S. Bell, P. A. Bertlmann, *Nucl. Phys.* **B187**, 285 (1981); *Phys. Lett.* **137B**, 107 (1984).
[32] W. Buchmüller, S.-H. H. Tye, *Phys. Rev.* **D24**, 132 (1981); W. Buchmüller, G. Grunberg, S.-H. H. Tye, *Phys. Rev. Lett.* **45**, 103, 587E (1980).
[33] L. Micu, *Nucl. Phys.* **B10**, 521 (1969).
[34] R. Carlitz, M. Kislinger, *Phys. Rev.* **D2**, 336 (1970); R. Feynman, M. Kislinger, F. Ravndal, *Phys. Rev.* **D3**, 2706 (1971).
[35] A. Le Yaouanc, L. Olivier, O. Pène, J. L. Raynal, *Phys. Rev.* **D8**, 2223 (1973).
[36] A. Mitra, M. Ross, *Phys. Rev.* **158**, 1630 (1967).
[37] J. Rosner, *Phys. Rev.* **D24**, 1347 (1981); **27**, 1101 (1983); J. Rosner, S. F. Tuan, *Phys. Rev.* **27**, 1544 (1983).
[38] M. Nicolic, *Phys. Rev.* **D26**, 3141 (1982); M. Schnitzer, *New Flavours and Hadron Spectroscopy*, Proc. of the 16th Rencontre de Moriond 1981, ed. J. Tran Thanh Van, Edition Francaise, France, p. 293.
[39] J. P. Ader, B. Bonnier, S. Sood, *Nuovo Cimento* **68A**, 1 (1981).
[40] A. Le Yaouanc, L. Olivier, O. Pène, J. C. Raynal, *Phys. Rev.* **D11**, 1272 (1975).
[41] M. Chaichian, R. Kögerler, *Ann. Phys.* (N.Y.) **124**, 61 (1980).
[42] V. Weisskopf, E. Wigner, *Z. Phys.* **63**, 54 (1930).
[43] Y. Dothan, D. Horn, *Phys. Rev.* **D1**, 916 (1970); C. Rebby, R. Slansky, *Phys. Rev.* **185**, 1838 (1969).
[44] J. L. Basdevant, E. L. Berger, *Phys. Rev.* **D19**, 239, 246 (1979).
[45] N. N. Achasov, S. A. Devianian, G. N. Schestakov, *Sov. J. Nucl. Phys.* **32** (4), 566, 1098 (1980); *Phys. Lett.* **88B**, 367 (1979).

[46] S. Flatté, *Phys. Lett.* **63B**, 224, 228 (1976).
[47] P. Kass, in: Proc. of the 19-th Rencontre de Moriond, Les Arcs, France, March 1984 (to be published).
[48] A. Silverman, Proc. of the 22-nd Int. Conference on High Energy Physics, Leipzig, July 19–25, 1984 (to be published).
[49] E. J. Squires, P. J. S. Watson, *Ann. Phys.* (N.Y.) **41**, 409 (1967).
[50] H. J. Lipkin, *Phys. Lett.* **72B**, 249 (1977).
[51] R. J. Jaffe, *Phys. Rev.* **D15**, 267, 281 (1977); Proc. of 1981 Symp. on Leptons and Photons at High Energy, ed. W. Pfeil, Bonn 1981, p. 395; R. L. Jaffe, F. E. Low, *Phys. Rev.* **D19**, 2105 (1979).
[52] N. Isgur, J. Weinstein, *Phys. Rev. Lett.* **48**, 659 (1982); *Phys. Rev.* **27**, 588 (1983).
[53] G. Zweig, (unpublished); P. Federman, H. R. Rubinstein, I. Talmi, *Phys. Lett.* **22**, 208 (1966).
[54] R. E. Cutcosky, P. Tarjanne, *Phys. Rev.* **132**, 1354 (1963).
[55] A. Katz, H. J. Lipkin, *Phys. Lett.* **7**, 44 (1963).
[56] J. Pasupathy, *Phys. Lett.* **58B**, 71 (1975); *Phys. Rev.* **D12**, 2929 (1975).
[57] G. F. Chew, C. Rosenzweig, *Phys. Rep.* **41**, 264 (1978).
[58] G. Fogli, G. Preparata, *Nuovo Cimento* **48A**, 235 (1978).
[59] A. K. A. Maciel, J. E. Paton, *Nucl. Phys.* **B181**, 277 (1981).
[60] W. N. Cottingham, K. Tsu, J. M. Richard, *Nucl. Phys.* **B179**, 541 (1981).
[61] F. Myhrer, G. E. Brown, Z. Xu, *Nucl. Phys.* **A362**, 317 (1981).
[62] A. W. Thomas, S. Théberge, G. A. Miller, *Phys. Rev.* **D24**, 2161 (1981).
[63] T. Hatsuda, *Prog. Theor. Phys.* **70**, 1685 (1983).
[64] E. Van Beveren, C. Dullemond, G. Rupp, *Phys. Rev.* **D21**, 773 (1980); E. Van Beveren, G. Rupp, T. A. Rijken, C. Dullemond, *Phys. Rev.* **D27**, 1527 (1973); E. Van Beveren, C. Dullemond, T. A. Rijken, *Z. Phys.* **C19**, 275 (1983).
[65] S. Jacobs, K. J. Miller, M. G. Olsson, *Phys. Rev. Lett.* **50**, 1181 (1983).
[66] T. N. Truong, *Acta Phys. Pol.* **B15**, 633 (1984); N. Deshponde, T. N. Truong, *Phys. Rev. Lett.* **41**, 1579 (1978); T. N. Truong, *Phys. Lett.* **99B**, 154 (1981).